

**Three-Dimensional Reconstruction of Friction Stir Welding  
Microstructure via Serial Sectioning**

by

Nurfatin binti Said

Dissertation submitted in partial fulfilment of  
the requirements for the  
Bachelor of Engineering (Hons)  
(Mechanical Engineering)

MAY 2011

Universiti Teknologi PETRONAS  
Bandar Seri Iskandar  
31750 Tronoh  
Perak Darul Ridzuan

# CERTIFICATION OF APPROVAL

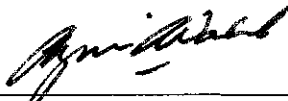
## Three-Dimensional Reconstruction of Microstructures via Serial Sectioning

by

Nurfatin binti Said

A Dissertation submitted to the  
Mechanical Engineering Programme  
Universiti Teknologi PETRONAS  
in partial fulfilment of the requirement for the  
BACHELOR OF ENGINEERING (Hons)  
(MECHANICAL ENGINEERING)

Approved by,



(Dr. Azmi Abdul Wahab)

Dr. Azmi Abd Wahab  
Lecturer  
Mechanical Engineering Department  
Universiti Teknologi PETRONAS  
Bandar Seri Iskandar, 31750 Tronoh  
Perak Darul Ridzuan, Malaysia.

UNIVERSITI TEKNOLOGI PETRONAS

TRONOH, PERAK

May 2011

## **CERTIFICATION OF ORIGINALITY**

This is to certify that I am responsible for the work submitted in this project, that the original work is my own except as specified in the references and acknowledgements, and that the original work contained herein have not been undertaken or done by unspecified sources or persons.

A handwritten signature in black ink, consisting of a large, stylized initial 'N' followed by several loops and a long horizontal stroke extending to the right.

---

NURFATIN BINTI SAID

## ABSTRACT

Three-Dimensional Reconstruction of Microstructures is one of the tools to reveal the patterns, shape, area that affected by processing condition. The objectives of this project are to perform serial sectioning as one of the technique of three-dimensional microscopy to generate three-dimensional microstructure image and to characterize the effect of friction stir welding on silicon carbide aluminum reinforced microstructure. Friction stir welding (FSW) has been successfully used to join aluminum matrix composites in a solid state joining process. The study of the microstructure of the weld joint typically involved common metallography preparation techniques, culminating in two-dimensional micrographs depicting the microstructure of the weld joint. The techniques of serial sectioning and three-dimensional reconstruction were employed to characterize the microstructure of silicon carbide (SiC) reinforced aluminum composite joined via the FSW process. Serial sectioning tasks were performed using conventional metallography techniques and equipment; however micrographs of the composite were recorded after each successive polishing step. Using the open source software NIH ImageJ, these micrographs were digitally enhanced and stacked to generate a 3D volume of the composite. The 3D reconstructions showed that a portion of the initial SiC particles were broken up by the FSW process and redistributed in the weld zone. Furthermore, the FSW process appeared to cause some of the unbroken SiC particles to align lengthwise in the welding direction. These characteristics would definitely influence the mechanical behaviour of the weld joint and future work will include the effects of welding parameters on the size and distribution of the SiC particles within the weld zone.

## **ACKNOWLEDGEMENTS**

First and foremost, I would like to praise God the Almighty for His guidance and giving me the strength to complete a Final Year Project (FYP) although difficulties and some dispute occurred. I would also like to take this opportunity to acknowledge and thank everyone that has given me all the support, guidance and facilities throughout the whole period of completing the project of ‘Three-Dimensional Reconstruction via Serial Sectioning’. My deepest appreciation goes to my supervisor, Dr. Azmi Abdul Wahab who has given me solid support and guidance with patience throughout the one year period of this final year project. He never stopped given me guidance and advices even though I have made some delays and mistakes upon completing the project. Credit to Mr. Umar Patthi a post graduate student who gave me some of his samples of the Friction Stir Welding aluminium composite apart being informative for every question I asked. that Besides that, I would like to thank the technicians from the Mechanical Engineering Department especially Mr. Irwan, Mr. Mahfuz and Mr. Shairul for helping me during the lab sessions in teaching me using the equipments in the lab. Finally, special thanks to my parents and family for their continuous love and support. Thank you.

## TABLE OF CONTENT

<b>CERTIFICATION OF APPROVAL</b> .....	i
<b>CERTIFICATION OF ORIGINALITY</b> .....	ii
<b>ABSTRACT</b> .....	iii
<b>ACKNOWLEDGMENT</b> .....	iv
<b>TABLE OF CONTENTS</b> .....	v
<b>LIST OF FIGURES</b> .....	vi
<b>LIST OF TABLES</b> .....	viii
<b>ABBREVIATIONS</b> .....	viii
<b>CHAPTER 1: INTRODUCTION</b> .....	10
1.1 Background Study.....	10
1.2 Problem Statement.....	11
1.3 Objectives.....	11
1.4 Scope of Study.....	11
<b>CHAPTER 2: LITERATURE REVIEW</b> .....	12
2.1 Three Dimensional Microscopy.....	12
2.2 Serial Sectioning.....	12
2.3 Friction Stir Welding on SCRA.....	13
<b>CHAPTER 3: METHODOLOGY</b> .....	17
3.1 Identification of Material .....	17
3.2 Sectioning .....	18
3.3 Mounting.....	19
3.4 Grinding.....	21
3.5 Polishing .....	23
3.6 Identification of Microstructure... ..	24
3.7 Serial Sectioning... ..	25
3.8 Milestone for FYP 1.....	31
3.9 Milestone for FYP 2.....	32
<b>CHAPTER 4: RESULTS AND DISCUSSION</b> .....	34
4.1 Characterization of Materials.....	34
4.2 Three Dimensional Reconstruction.....	37

<b>CHAPTER 5: CONCLUSIONS AND RECOMMENDATIONS</b> .....	45
5.1.1 Conclusions .....	45
5.1.2 Recommendations.....	45
<b>REFERENCES</b> .....	47
<b>APPENDICES</b> .....	49

### LIST OF FIGURES

Figure 2.1	Schematic sketch of FWS Process.....	14
Figure 2.2	: Macroscopic overview of the cross-section of the friction stir welded AA2124/SiC/25p composite to itself showing typical weld zones (Weld nugget, TMAZ, HAZ).....	15
Figure 2.3	Optical microstructures of the FSW joint of the composite: (a) Parent material; (b) heat affected zone (HAZ); (c) thermo-mechanical affected zone (TMAZ); and (d) weld nugget.....	15
Figure 2.4	SEM image of a polished cross-section of the weld nugget and EDX distribution maps of Si, C and Al in the same image.....	16
Figure 3.1	Flowchart of the process.....	17
Figure 3.2	Friction Stir Welded of SCRA Sample.....	18
Figure 3.3	Abrasive Cutter.....	19
Figure 3.4	Mounting Machine.....	20
Figure 3.5	(a) Diallyl-Phthalate Mineral Blue (b) : Release Agent being applied at the mold surface.....	21
Figure 3.6	Mounted Silicon Carbide Aluminum Sample.....	21
Figure 3.7	Grinding Machine.....	22

Figure 3.8	Automated Polishing Machine.....	24
Figure 3.9	Serial Sectioning Process Flowchart.....	25
Figure 3.10	(a) Microhardness Testing Machine (b) The fiducial mark being applied.....	26
Figure 3.11	Optical Microstructure.....	26
Figure 3.12	Fiducial mark diameter measurement.....	27
Figure 3.13	The first layer of the SCRA (a) In original color (b) 8 bit image.....	28
Figure 3.14	(a) Registry Plugin (b) Align Slice Plugin in ImageJ Software.....	28
Figure 3.15	Brightness and Contrast, Threshold plugin.....	29
Figure 3.16	3D Viewer.....	30
Figure 3.17	FYP 1 Milestone.....	31
Figure 3.18	FYP 2 Milestone.....	32
Figure 4.1	Micro-zones of the FSW.....	34
Figure 4.2	Optical microstructures of the FSW joint of the composite: (a) parent material; (b) heat affected zone (HAZ); (c) thermo-mechanical affected zone (TMAZ); and (d) weld nugget.....	36
Figure 4.3	SCRA Sample, where the red arrow indicted the direction of the welding and the area of interest.....	37
Figure 4.4	Series of Two-Dimensional Microstructure.....	37
Figure 4.5	Series of Two-Dimensional Microstructure.....	38
Figure 4.6	Series of Two-Dimensional Microstructure.....	39
Figure 4.7	(a) Positive XY Plane (b) Negative XY Plane.....	40
Figure 4.8	(a) Positive YZ Plane (b) Negative YZ Plane.....	40
Figure 4.9	(a) Positive XZ Plane (b) Negative XZ Plane.....	40

Figure 4.10	(a) (b): Three-Dimensional SCRA microstructure image.....	41
Figure 4.11	Another angle for the Three-Dimensional microstructure Image.....	42
Figure 5.1	(a) Sample polished using 1 micron diamond paste (b) Sample polished using 1 micron diamond past.....	46

### LIST OF TABLES

Table 3.1	Molding Temperature and Pressure used.....	20
Table 4.1	FSW Micro-zones SiC particle counts and average size.....	36
Table 4.2	Summary of FSW Weld Nugget coarse SiC particles distribution and size.....	43
Table 4.3	FSW Weld Nugget SiC particle counts and average size.....	43
Table 4.4	Summary of FSW Weld Nugget fine SiC particles distribution and size.....	44
Table 4.5	FSW Weld Nugget fine SiC particle counts and average size.....	44

### ABBREVIATIONS

FYP	Final Year Project
FSW	Friction Stir Welding
SCRA	Silicon Carbide Aluminum Reinforced
TWI	The Welding Institute
SZ	Stir Zone
TMAZ	Thermo-Mechanical Affected Zone

CDRX	“Continuous” Dynamic Recrystallization
HAZ	Heat Affected Zone
BM	Base Metal
EDX	Energy Dispersive X-Ray
SEM	Scanning Electron Microscope
SiC	Silicon Carbide

# **CHAPTER 1**

## **INTRODUCTION**

### **1.1 BACKGROUND STUDY**

Three-Dimensional Reconstruction of Microstructures is one of the tools used to reveal the patterns, shapes, and areas affected by alloy composition and processing condition [1] including cold working, heat treatment and welding. Three-Dimensional Microstructures reconstruction can also be used to detect defects that exist within a particular solid material because a finished part's environment can also affect its microstructure and cause problems such as corrosion and decarburization [2].

Friction-stir welding (FSW) is a solid-state joining process and is used for applications where the original metal characteristics must remain unchanged. This process is primarily used on aluminum where it cannot be easily heat treated post weld to recover temper characteristics. The solid-state nature of the FSW process, combined with its unusual tool and asymmetric nature, results in a highly characteristic microstructure [3].

### **1.2 PROBLEM STATEMENT**

Friction-stir Welding is a joining process of the metals where the metal endures solid state processing condition. In this project, the material studied is silicon carbide reinforced aluminum composite. This processing condition affects the microstructure of the alloy and it is important to analyze the condition of the microstructure to decide the right material for the right applications. Typical observations of microstructures are usually performed using two-dimensional

micrographs. Often the true representation of the materials is rarely observed due to the simplicity of the two-dimensional information. Additionally, actual three-dimensional microstructural features have to be inferred from these 2-D images. Means of creating 3-D microstructural images are thus needed and the real image of the structures would be obtained enabling precise analyses and gathering of information of the material structure.

### **1.3 OBJECTIVES AND SCOPE OF STUDY**

The main objectives for this project are:

- To obtain sequential microstructure of the Friction Stir Welding
- To characterize the microstructure of the Friction Stir Welding
- To perform serial sectioning as one of the technique of Three-Dimensional Microscopy
- To generate Three-Dimensional images from serial sectioning.

The scope of work for this project is to generate three-dimensional reconstruction of the Friction Stir Welding Silicon Carbide Reinforced Aluminum. There are many *techniques* to generate the three-dimensional microscopy which include serial sectioning, x-ray tomography, electrolytic dissolution and focused ion beam ablation [1]. This project will be focusing on serial sectioning technique that capable to produce sequential micrographs at either 0.5 or 1.0 micron intervals. These images will be digitally processed to create 3-D reconstruction of the volume using ImageJ software.

## **CHAPTER 2**

### **LITERATURE REVIEW**

#### **2.1 THREE-DIMENSIONAL MICROSCOPY**

Three-Dimensional reconstruction of Microscopy is the method that reveals the shape, patterns, distribution and connectivity of three-dimensional (3D) features that are hidden within a solid material [1]. The variety of three-dimensional (3D) visualization techniques used in medical application gives scientists the thought, necessity, and desire to reveal hidden internal structures and connectivity in materials. The traditional two-dimensional (2D) metallographic methods provide single and polished-and-etched sections for observation. This method being applied quantitatively to estimate some parameters that describe 3D features of polycrystalline or multiphase materials [2, 5].

In conventional metallography, based on the observations of single polished and etched sections, certain assumptions are made about the shapes of 3D features that lie buried within a specimen. In most simple cases, the shapes of many simple features can be accurately deduced using this approach. However, when the case involves sizes, spatial distributions, shapes, and interconnectivities of more complicated microstructures, the features can only be characterized with 3D analysis [12].

#### **2.2 SERIAL SECTIONING**

Three-Dimensional reconstruction techniques include Serial Sectioning, Focused Ion Beam Tomography, Atom Probe Tomography, X-Ray Microtomography and Computer Reconstruction and Visualization of Three-Dimensional Data. This project will apply specifically the Serial Sectioning technique to reconstruct three-dimensional features in order to observe the effect of

Friction Stir Welding on Silicon Carbide Reinforced Aluminum (SCRA). Recent improvements in image processing and 3D visualization capabilities in addition to the development of automatic sectioning devices have made 3D reconstruction and visualization of serial sections much more practical.

To overcome the limitations of the intrinsic two-dimensional nature of electron microscopy, sections can be cut serially from the specimen. Each section contains a portion of the original structure that can be separately imaged with transmission electron microscopy. In the pre-computer era, tracings of sectioned objects were transferred to physical material and assembled to reconstruct the three-dimensional structure from the section images [8].

Serial sectioning techniques is the process the material from bulk sample layer by layer will be removed and the reconstructing the resultant series images using computer program. The basic serial-sectioning material-removal methods involve manual or semi-automated polishing which can remove between approximately 0.05 and 1.0  $\mu\text{m}$ /section and micromilling (which removes between approximately 0.05 and 1.0  $\mu\text{m}$ /section). Other experimental parameters that maybe applicable include the number of section required, whether an etchant is required, the use of fiducial marks, imaging method, image acquisition and visualization software [12].

### **2.3 FRICTION STIR WELDING ON SILICA CARBIDE REINFORCED ALUMINUM**

Friction-stir welding (FSW) is a solid-state joining process where it undergoes friction heating combined with forging pressure to produce high-strength bonds with virtually no defects. This technique was invented by The Welding Institute (TWI) in 1991. Friction Stir Welding transforms the metals from a solid state to a “plastic like” state [4] and mechanically stirs the material together under pressure to form a welded joint. It does not require the need for gas shielding or filler metals and is also an improved and faster way of producing aluminum joints [9,

10]. Friction-stir Welding can be described in conventional terms as a combination of extrusion and forging of metal at elevated temperature [10].

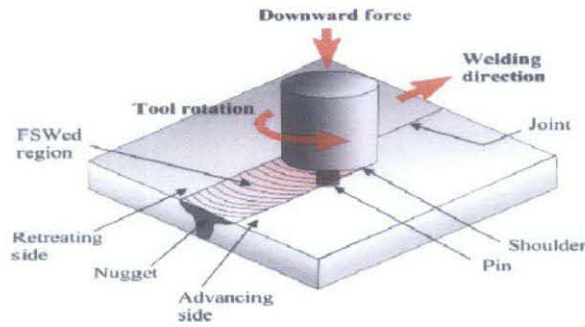


Figure 2.1: Schematic sketch of FWS Process [6]

The low mechanical properties microstructure resulting from melting and re-solidification are absent in FSW welds, leading to improved mechanical properties such as high ductility and high strength alloys with low residual stresses. The application of FSW technology is in particular dependent on mechanical performances affected by the processing parameters. The mechanical properties were evaluated by means of tensile and fatigue tests at room temperature for different welding conditions.

Friction Stir Welding process is where a non-consumable tool with a specially designed rotating pin is entered into abutting edges of a sheet or plate to be welded. Once entered, the rotating tool produces frictional heat and plastic deformation in the specimen. The tool is then translated along the joint to complete the joining process. Frictional heat and plastic flow during friction stir welding create the fine recrystallized grain (Stir Zone, SZ) and the elongated and recovered grain (Thermo-Mechanical Affected Zone, TMAZ) in the weld zone [6].

The stir zone (also called nugget) is a region of heavily deformed material that roughly corresponds to the location of the pin during welding. Thus, it makes the stir area (nugget) relevant to be studied and constructed the three dimensional micrograph. The grains within the stir zone are roughly equiaxed and often an order of magnitude smaller than the grains in the parent material [3]. The micro structural evidence suggests that a “continuous” dynamic recrystallization (CDRX) process

occurs, caused by the tool pin stirring action. In FSW, the thermo-mechanical action of the tool pin determines grains breaking down to a microstructure characterized by very fine, equiaxed grains [7]. The FSW grain structure and the microstructure of the nugget can be seen in Figure 2.3 and Figure 2. 4.

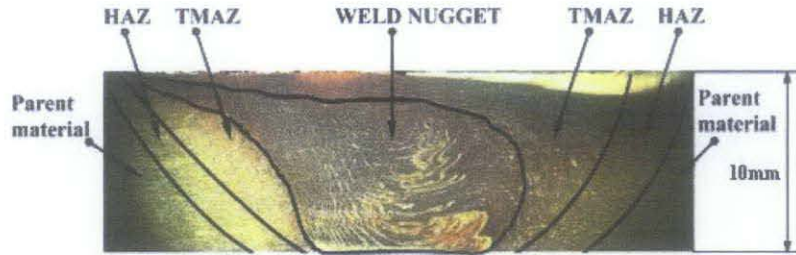


Figure 2.2: Macroscopic overview of the cross-section of the friction stir welded AA2124/SiC/25p composite to itself showing typical weld zones (Weld nugget, TMAZ, HAZ) [14].

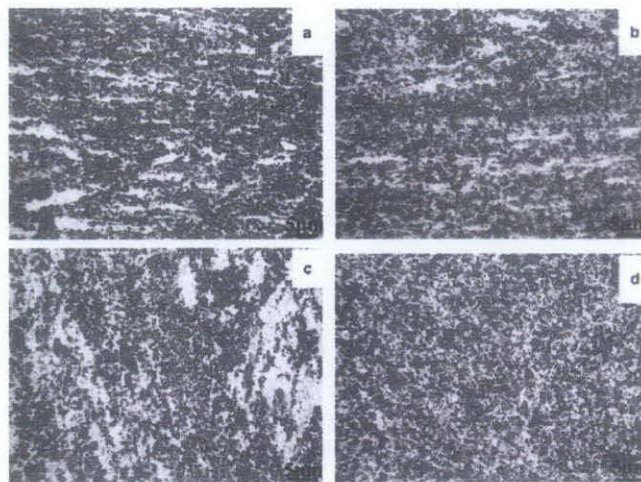


Figure 2.3: Optical microstructures of the FSW joint of the composite: (a) parent material; (b) heat affected zone (HAZ); (c) thermo-mechanical affected zone (TMAZ); and (d) weld nugget [14].

The thermo-mechanically affected zone (TMAZ) has been plastically deformed and thermally affected that cause the elongation of the Al alloy matrix and the SiC particle free regions of the composite. However, the heat affected zone (HAZ) exhibits a microstructure similar to the base metal of the aluminum composite. The distribution of the SiC particles in the nugget region is more homogeneous, suggesting the re-arrangement of the particles had occurred during friction stir welding due to the high deformation and stirring [14].

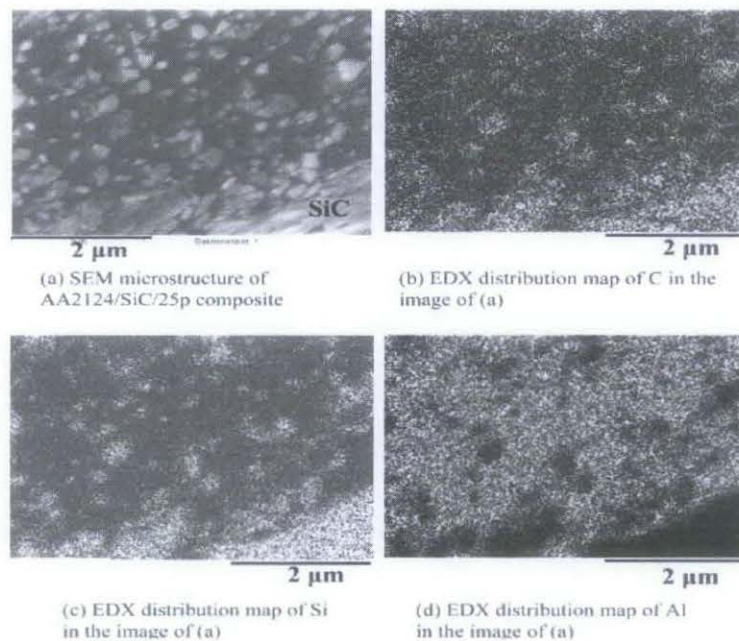


Figure 2.4: SEM image of a polished cross-section of the weld nugget and EDX distribution maps of Si, C and Al in the same image [14].

Figure 2.4 illustrates the SEM image where the Si, C and Al distributions analyzed by EDX consisted with the SEM image reveal the presence of fine and coarse SiC particles in the weld nugget and base composite.

## CHAPTER 3

### METHODOLOGY

The general process flow for this project is shown in Figure 3.1, whereas the flowchart for the serial sectioning process is shown in Figure 3.9.

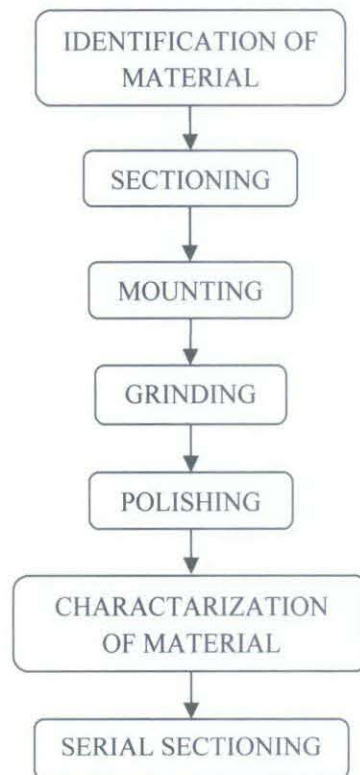


Figure 3.1: Flowchart of the process

#### 3.1 IDENTIFICATION OF MATERIAL

The process started with the identification of the material which is friction stir welded Silicon Carbide Reinforced Aluminum and the area of interested was determined which is the weld nugget area where it is subjected to the friction stir welding process.

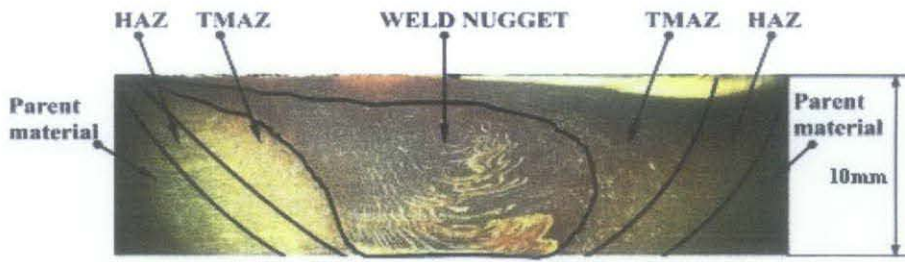


Figure 3.2: Friction Stir Welded of SCRA Sample

### 3.2 SECTIONING

Sectioning is the removal of a representative sample from parent piece while the microstructure must not be altered in the process. Heat or cold working is the two most likely conditions which would quickly bring about the structure changes. It is apparent that operations like sawing or shearing are not preferable due to severe deformation produced. Thus abrasive cutting offers the best solution to eliminate or minimize heat and deformation [2, 6].

The area of interest was cut by using the abrasive cutter and to cut properly, a bonded abrasive wheel must be matched to the cutoff machine. Primary considerations are surface speed (SFM) for a given wheel diameter and the type of cooling system employed. Sufficient and proper cooling during cutting process is extremely important [2]. High-volume jet spraying or submerged cutting are the two major techniques used. But in this project, jet spraying being employed throughout the cutting process because submerged cutting will tend to make a wheel bond act harder.

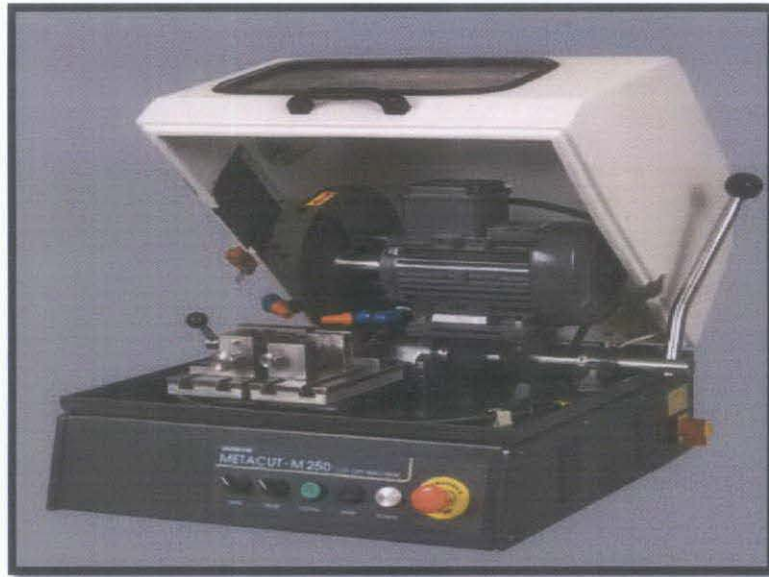


Figure 3.3: Abrasive Cutter [15]

### 3.3 MOUNTING

Metallographic samples were mounted primarily for ease in manipulation and for edge retention during preparation. Compression molding technique is used to produce hard mounts in minimum of time. The materials used are classified in two categories which are thermosetting and thermoplastic. Thermosetting media requires heat and pressure during the molding cycle and can be ejected at maximum molding temperature. Thermoplastic materials remain fluid at maximum molding temperatures and become dense and transparent with a decrease in temperature and an increase in pressure.

The sample in this project was mounted using the thermosetting materials (Figure 3.6). This practice is recommended as powdered materials has an extremely large exposed surface area and consequently the individual grains, upon contact with heated molds, have marked tendency to immediately cure without fusion. Pre-molded thermoset performs can be used when a section will not be damaged as it is forced into the mounting material by initial application of pressure [2, 6].



Figure 3.4: Mounting Machine

Table 3.1: Molding Temperature and Pressure used

<b>Classification</b>	Thermosetting
<b>Molding Material</b>	Diallyl-Phthalate Mineral Blue
<b>Molding Temperature (°F)</b>	300-360
<b>Molding Pressure (psi)</b>	4000
<b>Heating Time (minute)</b>	3
<b>Cooling Time (minute)</b>	5
<b>Release Agent Requirement</b>	Yes

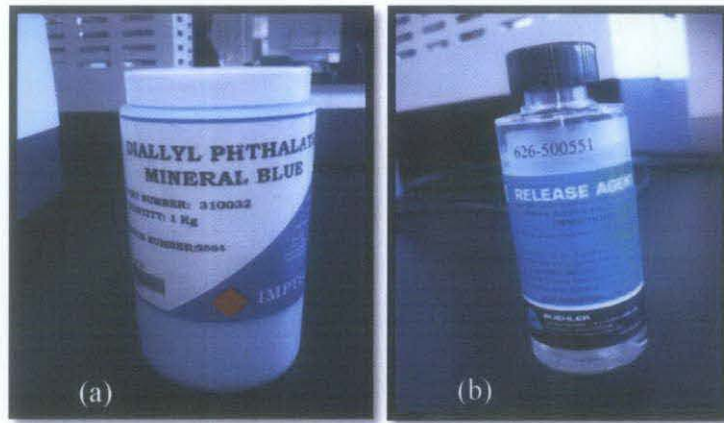


Figure 3.5:(a) Diallyl-Phthalate Mineral Blue (b) : Release Agent being applied at the mold surface

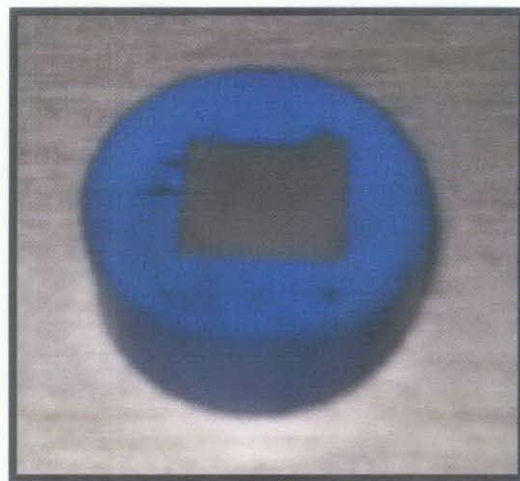


Figure 3.6: Mounted Silicon Carbide Aluminum Sample

### 3.4 GRINDING

Coarse grinding produces an initial flat surface. The purpose of coarse grinding is to remove deformation produced during sectioning and provide the initial flat surface. The other purpose may often be to remove gross amounts of surface material for microsample preparation or macroetching [2, 6]. However, this coarse grinding process is not necessary since the sample after the mounting process produces a flat surface and jumps to the fine grinding process.

The purpose of fine grinding is to remove the zone deformation caused by sectioning and coarse grinding and limit the depths of deformation during this stage.

by proper abrasive size quenching [2, 6]. The fine grinding process was started with the 240 grit, 320 grit, 400 grit and 600 grit respectively. The speed of the fine grinding was adjusted depending on the person's dexterity. This is because the abrasive action is very aggressive with higher speed fine grinding (increased surface feet per minute) and resulting surface finish for a given grit size will approach that produced by a finer grit size.

- 240 grit
- 320 grit
- 400 grit
- 600 grit

With semi manual fine grinding process, the sample was firmly held with the fingers and one finger pressing in the middle of the sample to provide sufficient and uniform pressure. The sample was held adequately firm and avoiding putting too much pressure that may cause faceting and scratch to the sample. Too loose in holding the sample can cause the sample flying away from the grinder surface and may cause injury to the person or damaging the grinding machine and scratching the sample surface.



Figure 3.7: Grinding Machine

### 3.5 POLISHING

Rough polishing is the further limitation of the deformation zone produced by fine grinding while final polishing is the removal of deformation zone produced during rough polishing. This considered the most important in the entire preparation sequence. Polishing process requires abrasive and the abrasives used in this project were 9 micron, 1 micron and 0.25 micron diamond abrasive or also known as diamond paste. The nature of the abrasive type employed should permit accurate sizing and separation by various methods into fractions of uniform particle size. Diamond particles retain their shape and size during abrasion and produce a uniform and high rate of material removal with minimal induced surface damage (2).

The 1 micron diamond paste was applied on the sample surface and polished using the automated polishing machine as shown in Figure 3.8. The paste-like material enhances convenient charging of the polishing cloth surface, and the addition of an extender contributes to even particle distribution over the surface. The sample surface will naturally show scratches of visible dimensions and there will be localized deformation associated with these scratches. The sample was polished from 9 micron, 1 micron and 0.25 micron respectively to prepare the sample to be analyzed under the optical microstructure.

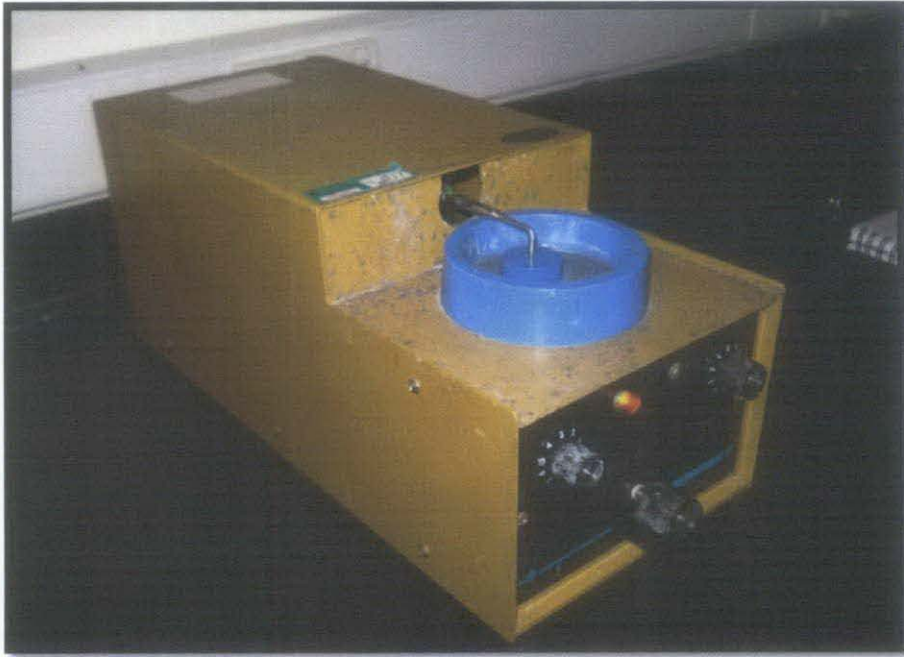


Figure 3.8: Automated Polishing Machine

### 3.6 IDENTIFICATION OF MICROSTRUCTURE

The process continued with the identification of microstructure once the sample preparation is completed with the usage of optical microscope. The process of characterization of the material started with the 50 magnification, 100 magnifications, 500 magnifications, 1000 magnifications and 1500 magnifications respectively. The images were taken from different spots to ease the characterization process.

### 3.7 SERIAL SECTIONING

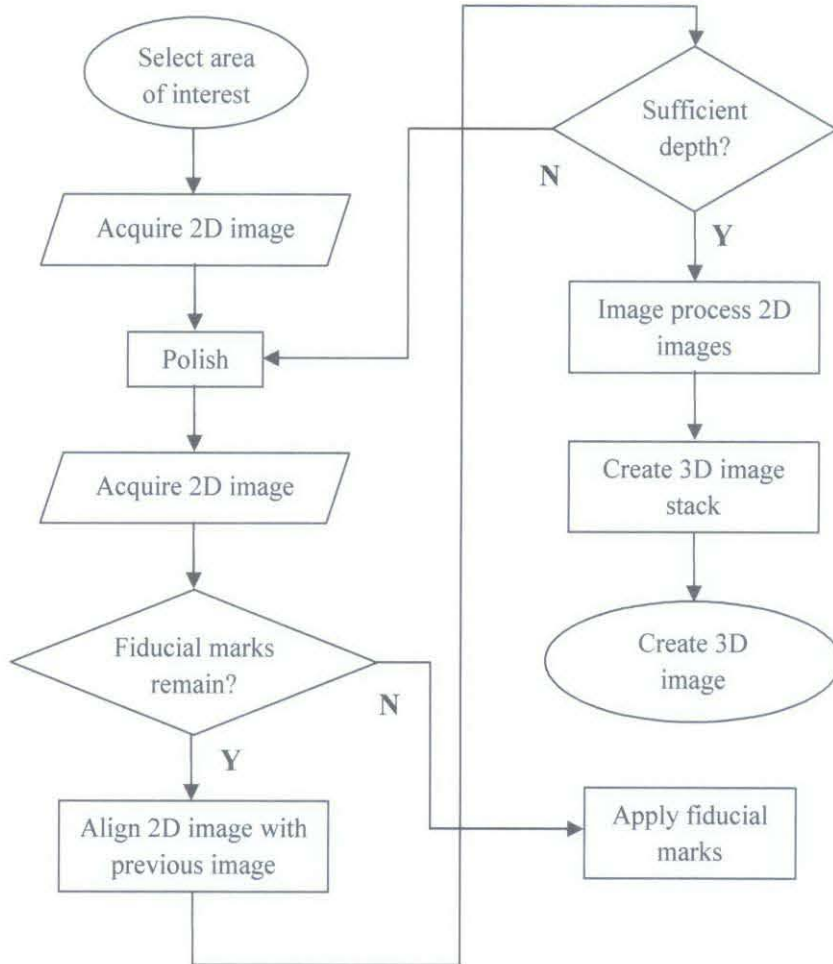


Figure 3.9: Flowchart of the serial sectioning process

Proceeded with the serial sectioning process where the area of interest was selected and fiducial marks were applied using the microhardness testing equipment. The fiducial marks acted as indicator of the thickness of layer being removed during the serial sectioning process.

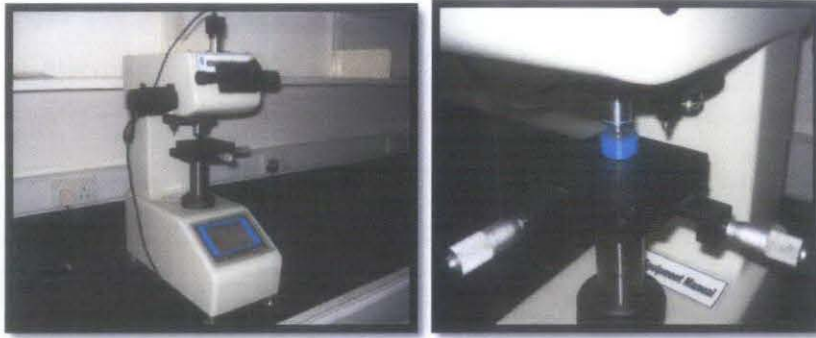


Figure 3.10: (a) Microhardness Testing Machine (b) The fiducial mark being applied

After the fiducial marks were applied, the diameters of the fiducial marks were recorded and the two-dimensional image was captured using the optical microstructure (Figure 3.11). The magnification used for the serial sectioning process is 500 magnifications.



Figure 3.11: Optical Microstructure

Then the sample was polished for approximately 10 minutes for the 1 micron thickness to be removed. However, the thickness removed depending on the condition of the polishing cloth. The polishing time will increase slightly for about 12 to 13 minutes if the polishing cloth is about to worn off. The polishing cloth was changed from time to time when the polishing cloth is worn off.

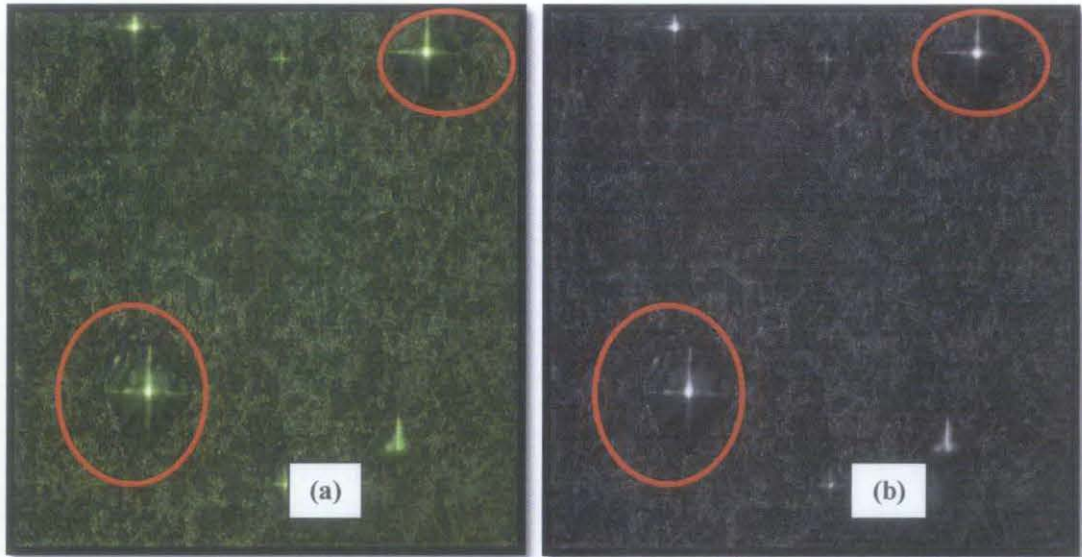


Figure 3.13: The first layer of the SCRA (a) In original color (b) 8 bit image

There were some layers that failed to be aligned by the register plugin, were aligned manually using the align slice plugin in the ImageJ software (Figure 3.14). This problem occurred probably due to the images being used contains too many tiny spots where the software confused with the actual SiC particles of interests in this project.

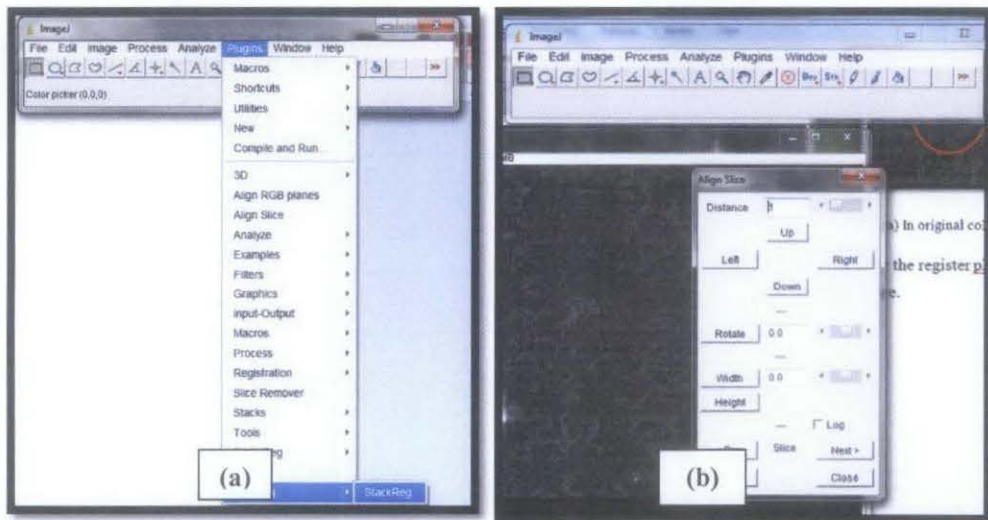


Figure 3.14: (a) Registry Plugin (b) Align Slice Plugin in ImageJ Software

After all 50 images were aligned, those images were adjusted its brightness and contrast to prepare the images to be threshold (Figure 3.15). Threshold process is where point that must be exceeded to begin producing results, in this case the three-dimensional microstructure image. Those images were cropped to eliminate the fiducial marks from appearing in the three-dimensional viewer or 3D Viewer (Figure 3.16).

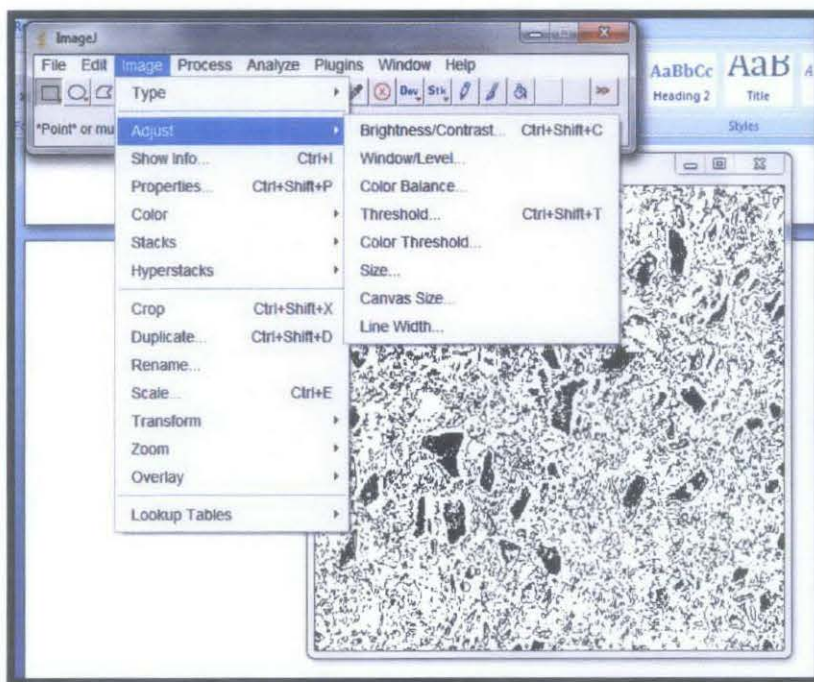


Figure 3.15: Brightness and Contrast, Threshold plugin

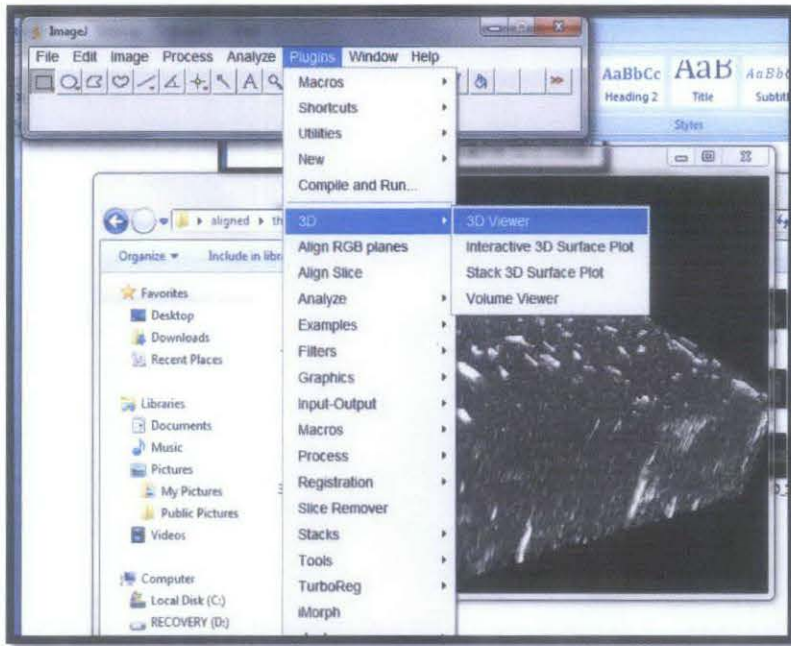


Figure 3.16: 3D Viewer

The three-dimensional microstructure images were captured from six different angles using the 3D Viewer plugin for the complete view of the microstructure. The complete view of the three-dimensional microstructure is important for full inspection of the Silicon Carbide particles distribution, shape and sizes.

### 3.8 MILESTONE FOR FINAL YEAR PROJECT 1

No	Detail/Week	1	2	3	4	5	6	Mid-Semester Break		7	8	9	10	11	12	13	14
1	Selection of Project Topic	■	■														
2	Preliminary Research Work		■	■	■												
3	Submission of Preliminary Report				●												
4	Project Work																
	- Identification of Material					■											
	- Sectioning						■										
5	Submission of Progress Report										●						
6	Seminar										●						
7	Project Work Continues																
	- Mounting									■							
	- Grinding										■	■					
	- Polishing											■	■				
	- Characterization of Material													■	■		
	- Serial Sectioning															■	■
8	Submission of Interim Report Final Draft																●
9	Oral Presentation																

Figure 3.17: FYP 1 Milestone

### 3.9 MILESTONE FOR FINAL YEAR PROJECT 2

No	Detail/Week	1	2	3	4	5	6	7	8	9	10	11	12	13	14	15	
1	Project Work Continues							MID-SEMESTER BREAK									
	- Serial Sectioning up to 30 layers.																
2	Submission of Progress Report									●							
3	Project Work Continues																
	- Serial Sectioning for the remaining 20 layers.																
	- Generate 3-D images by using ImageJ																
4	Pre-EDX												●				
5	Submission of Draft Report													●			
6	Submission of Dissertation (Soft Bound)														●		
7	Submission of Technical Paper													●			
8	Oral Presentation														●		
9	Submission of Project Dissertation (Hard Bound)															●	

Figure 3.18: FYP 2 Milestone

- **Suggested Milestone**
- **Process**

Figure 3.17 and 3.18 show the project activities for the two semesters. These milestones act as a guideline for the project activities and documentation deadlines. Basically, milestone for Final Year Project 1 (FYP 1) is the series of steps (refer to Figure 3.1) to characterize the microstructure and to prepare the sample for the serial sectioning process. While milestone for Final Year Project 2 (FYP 2) is the activities of the serial sectioning (refer to Figure 3.9) to generate three-dimensional microstructure and to further characterize the microstructure distribution.

## CHAPTER 4

### RESULTS AND DISCUSSION

#### 4.1 CHARACTERIZATION OF THE MATERIALS

Friction stir welding weld zones divided up to four distinct micro-zones based on microstructural characterization by optical microscopy information. These zones are identified as weld nugget, thermo-mechanically affected zone (TMAZ), heat affected zone (HAZ) and parent material or basemetal (BM) as shown in Figure 4.1. Specimen was sectioned from the plate and the transverse face was polished to a 0.25 micron finish for the optical microscopy characterization. Several different microstructures were observed within the weld as the result of friction stir welding process.

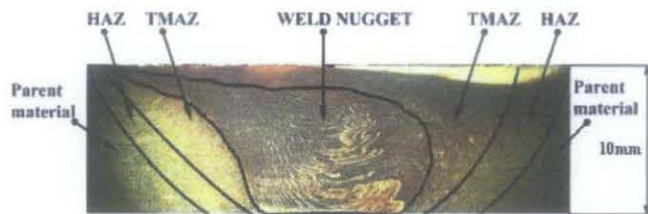


Figure 4.1: Micro-zones of the FSW [14]

Table 4.1 shows summarized results run by the ImageJ software to analyze the distribution and also the size of the silicon carbide particles in each micro-zone. The values shown in the Table 4.1 are the silicon carbide particles average counts and the average size for fine and coarse particles. In general, the optical microstructure for the parent material the silicon carbide composite particle is almost uniformly distributed as shown in Figure 4.2 (a). The silicon carbide particles are

greatest in average size with average 5.598  $\mu\text{m}$  coarse particle size based and the least fine particles count compare to the heat affected zone (HAZ), thermo-mechanically affected zone (TMAZ) and the weld nugget area as tabulated in Table 4.1 below.

The heat affected zone (HAZ) Figure 4.2 (c) has particle size ranging from 0.1  $\mu\text{m}$  to 0.3  $\mu\text{m}$  for fine particles and 2  $\mu\text{m}$  to 4  $\mu\text{m}$  for coarse particles. This probably attributed to the stirring action during the friction stir welding process where the silicon carbide particles break into tinier pieces. The thermo-mechanically affected zone (TMAZ) has been plastically deformed and thermally affected where the silicon carbide particle is elongated. Thus, it affects the silicon carbide distribution and sizes as shown in Figure 4.2 (c) where the particles being finer than the base metal area. However, the heat affected zone (HAZ) and the thermo-mechanically affected zone (TMAZ) silicon carbide particle distribution are both relatively similar except the thermo-mechanically affected zone (TMAZ) silicon carbide particle size being slightly smaller average size than the heat affected zone (HAZ).

The weld nugget zone Figure 4.2 (d), exhibits the greatest count for the fine particles and the least count for the coarse particles. The stirring effect cause the coarse silicon carbide particle from the parent metal mixed with the finer silicon carbide particle that mainly concentrated at the heat affected zone (HAZ). The silicon carbide particle also elongated at the weld nugget zone as the result from the stirring effect.

Table 4.1: FSW Micro-zones SiC particle counts and average sizes.

MICRO-ZONES	COUNT		AVERAGE SIZE ( $\mu\text{m}$ )	
	Fine	Coarse	Fine	Coarse
Base Metal (BM)	168	189	0.287	5.598
Heat Affected Zone (HAZ)	350	181	0.317	4.546
Thermo-Mechanically Affected Zone (TMAZ)	416	190	0.319	4.466
Weld Nugget	465	95	0.297	4.515

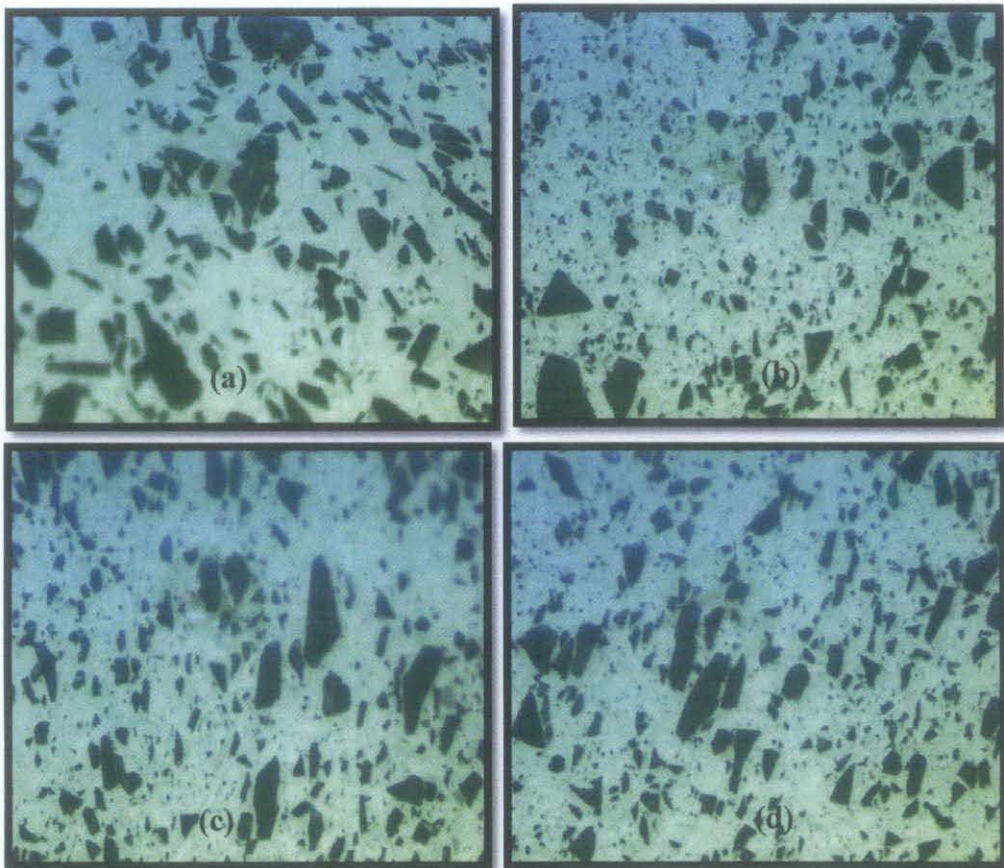


Figure 4.2: Optical microstructures of the FSW joint of the composite: (a) parent material; (b) heat affected zone (HAZ); (c) thermo-mechanical affected zone (TMAZ); and (d) weld nugget.

## 4.2 THREE DIMENSIONAL RECONSTRUCTION

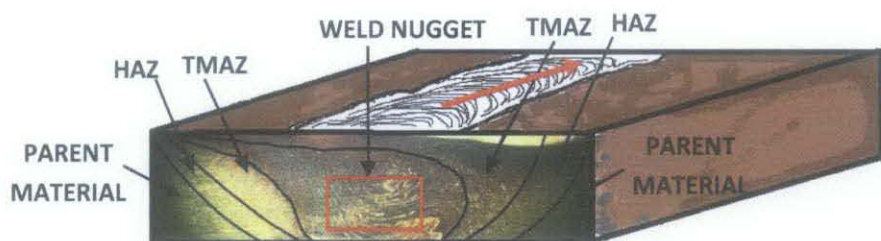


Figure 4.3: SCRA Sample, where the red arrow indicated the direction of the welding and the area of interest.

The 50 images were all stacked, aligned and threshold by using plugins in the ImageJ software (stackreg or registry and 3D Viewer).

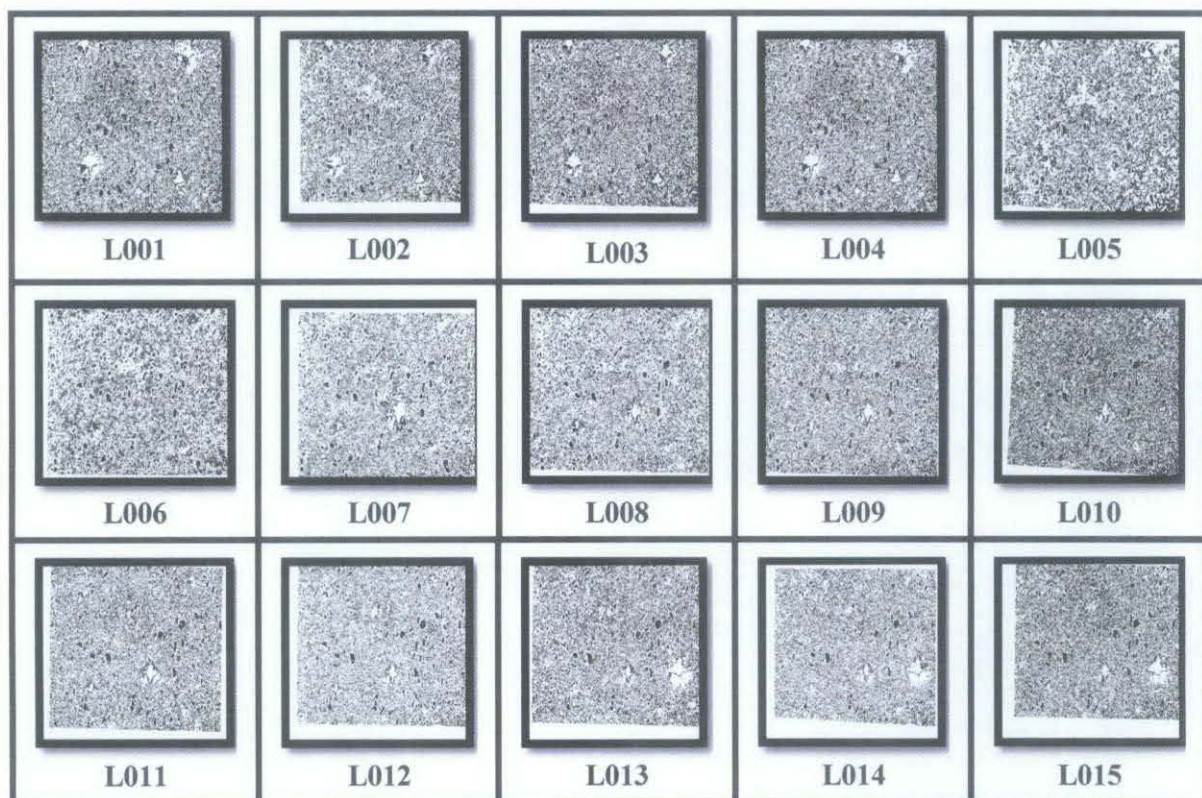


Figure 4.4: Series of Two-Dimensional Microstructure



Figure 4.5: Series of Two-Dimensional Microstructure

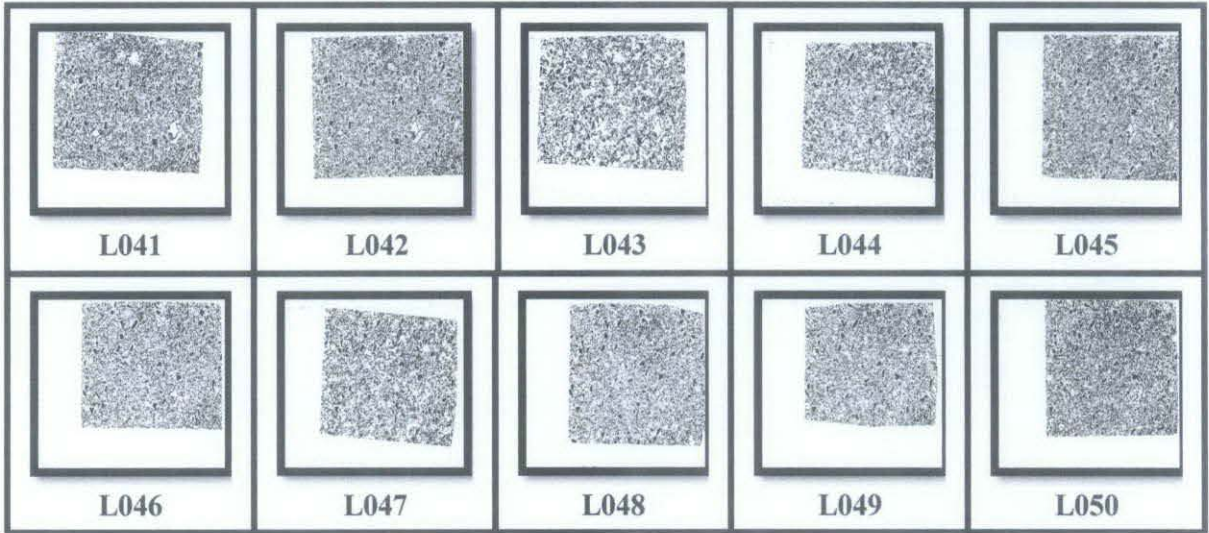


Figure 4.6: Series of Two-Dimensional Microstructure

Series of images in Figure 4.4, 4.5 and 4.6 were stacked and three-dimensional microstructure generated. The generated three-dimensional microstructure image was captured in six different plane which are positive XY plane (Figure 4.7 (a)), negative XY plane (Figure 4.7 (b)), positive YZ plane (Figure 4.8 (a)), negative YZ plane (Figure 4.8 (b)), positive XZ plane (Figure 4.9 (a)) and negative XZ plane (Figure 4.9 (b)).

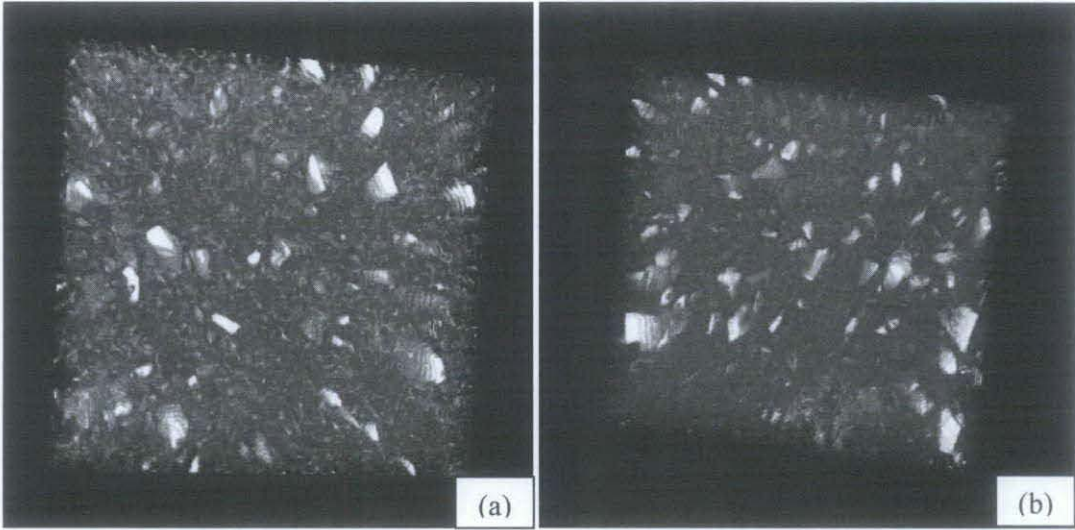


Figure 4.7: (a) Positive XY Plane (b) Negative XY Plane

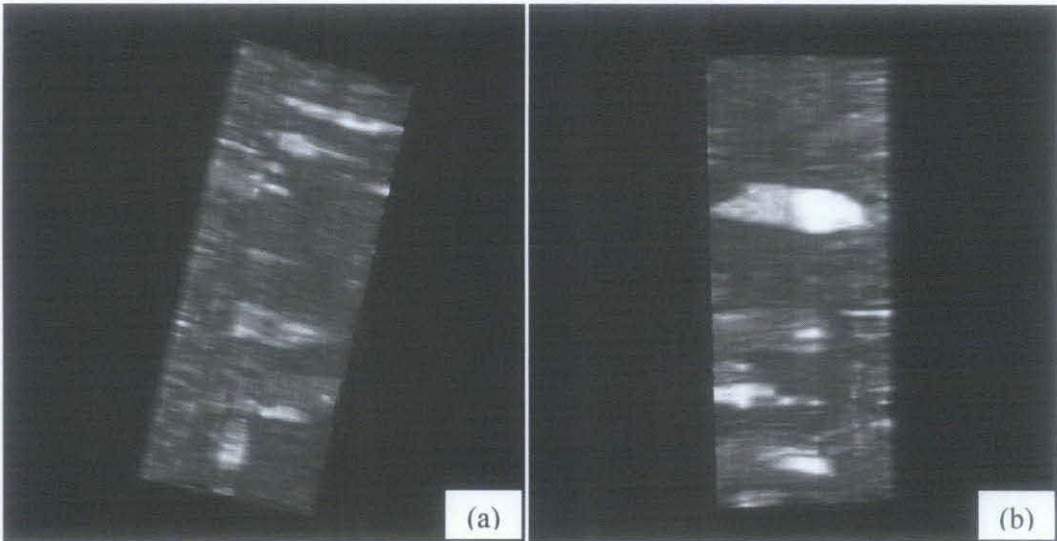


Figure 4.8: (a) Positive YZ Plane (b) Negative YZ Plane

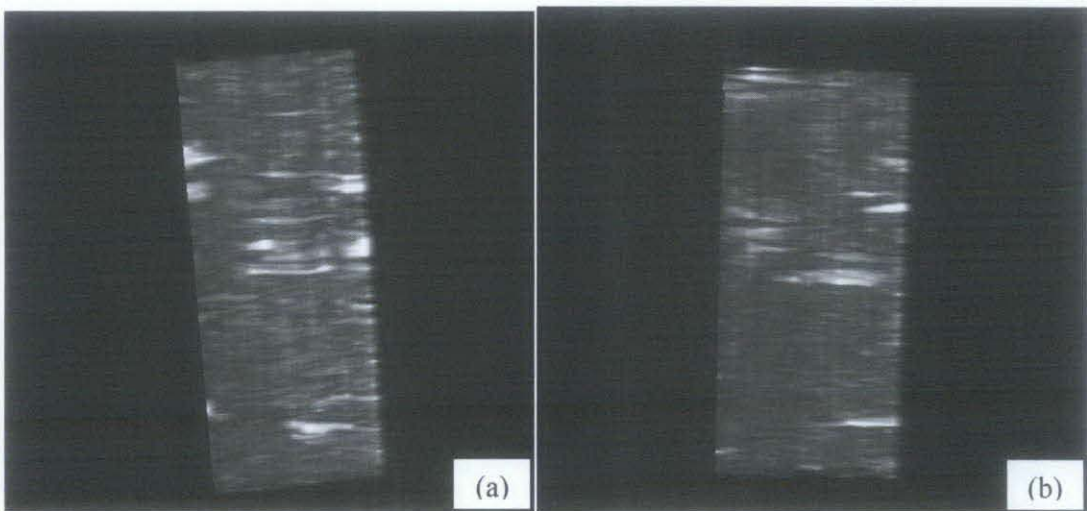


Figure 4.9: (a) Positive XZ Plane (b) Negative XZ Plane

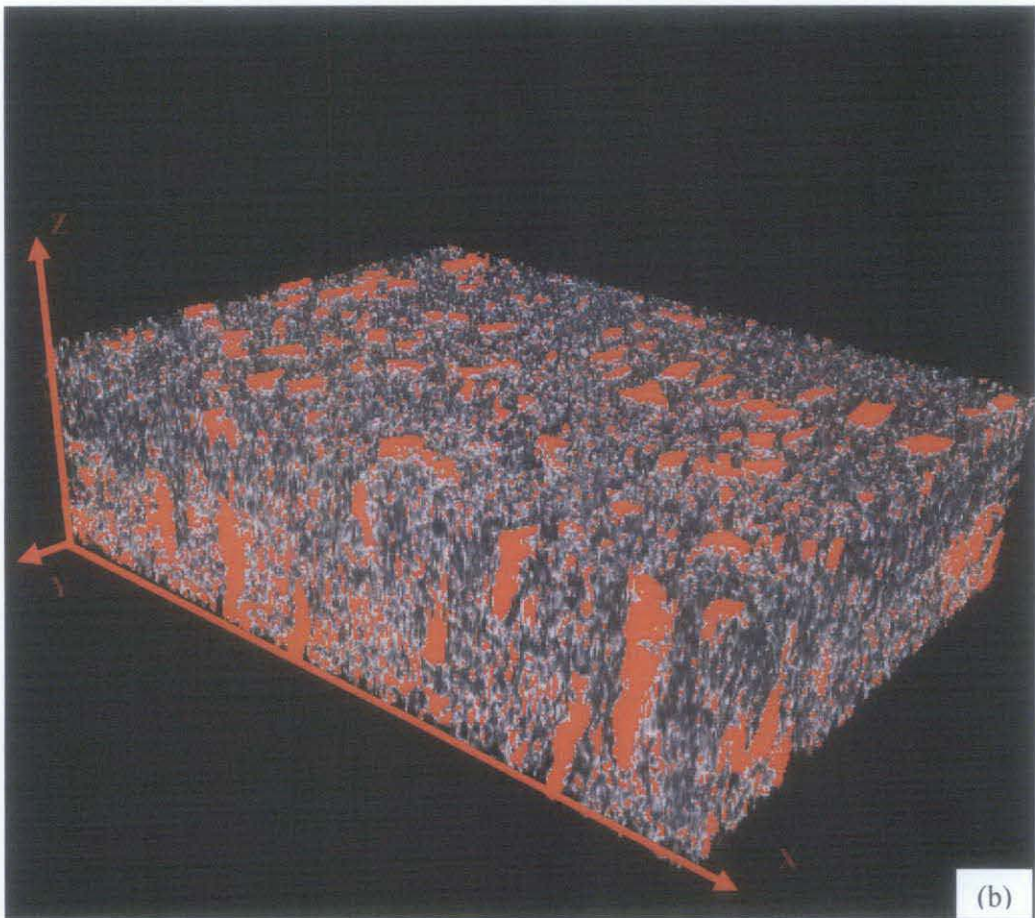
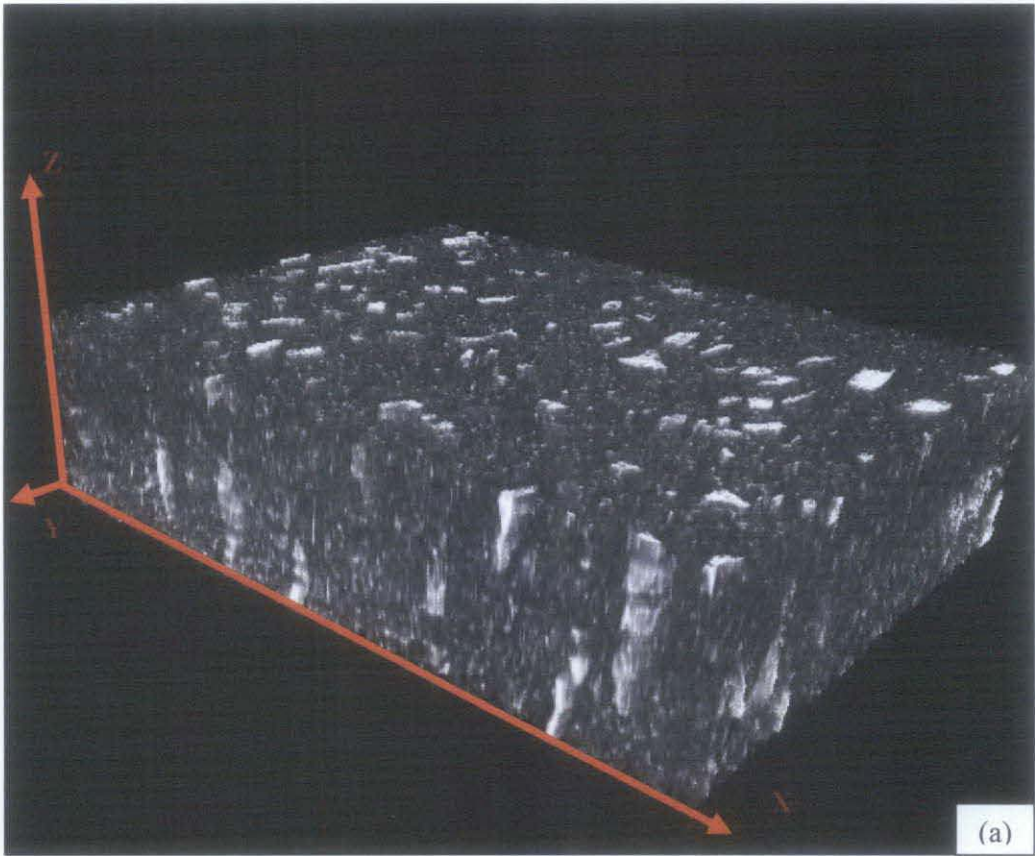


Figure 4.10(a) (b): Three-Dimensional SCRA microstructure images

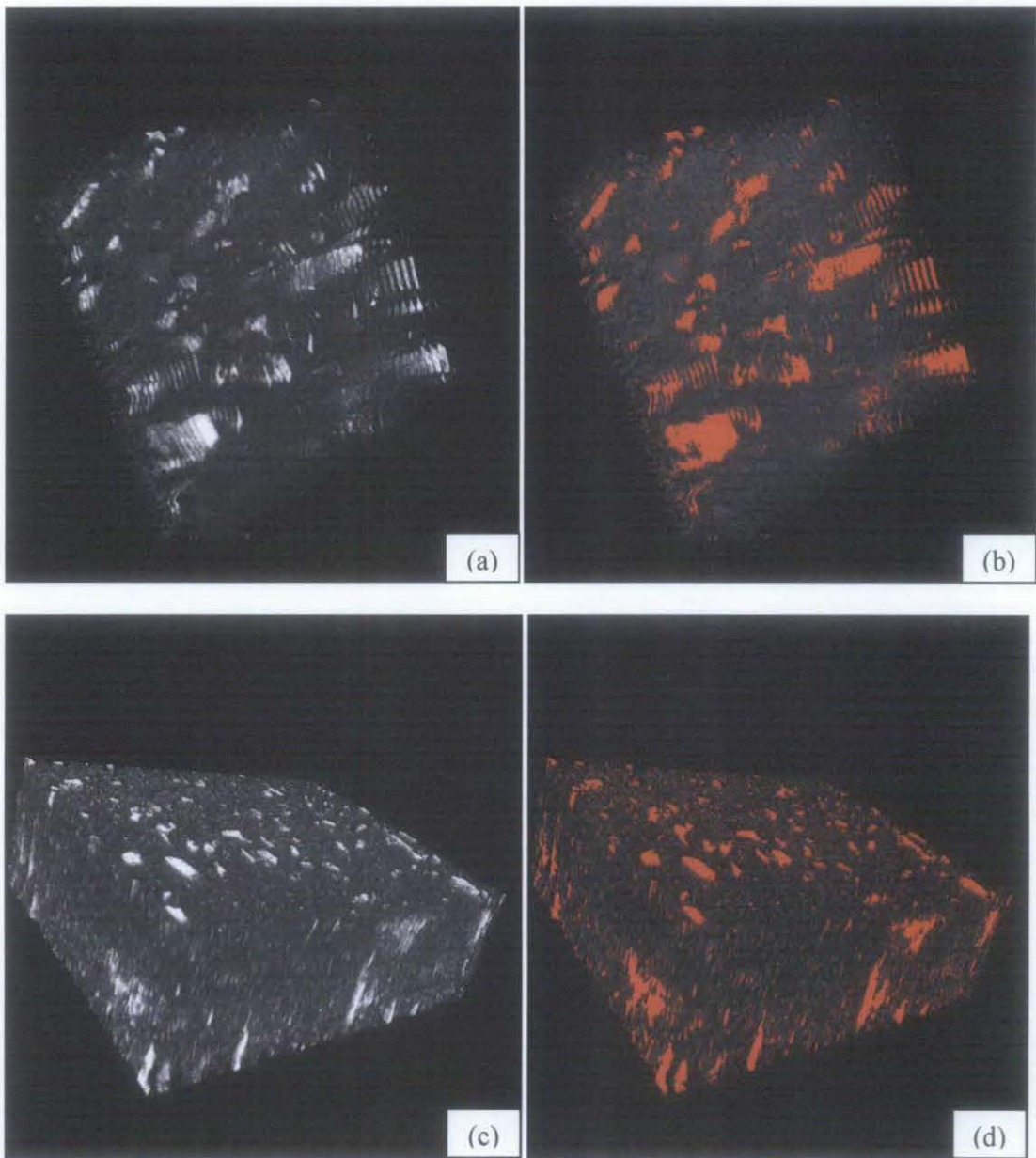


Figure 4.11: Another angle for the Three-Dimensional microstructure images

The three-dimensional microstructure friction stir welded of SCRA are shown in Figure 4.10 and 4.11. From the three-dimensional image generated, the SiC particles distribution is almost uniform and more homogeneous. This indicating that re-arrangement of the particles had taken place during friction stir welding due to the high deformation and stirring. However, the SiC particles were elongated in the Z direction along with the friction stir welding direction as indicated in Figure 4.10 (b), where the SiC particles are distinguished in red color. The friction stir welding process causes the SiC particles to elongate and formation of the fine SiC particles.

Table 4.2 shows the summarized data of the coarse SiC particles distribution and size. The particles measurement was analyze using ImageJ. The weld nugget consist coarse SiC particles between 1 and 10 micron. The average count and the average size of the SiC particles in the three-dimensional microstructure are tabulated in Table 4.3.

Table 4.2: Summary of FSW Weld Nugget coarse SiC particles distribution and size

Slice	Count	Total Area ( $\mu\text{m}^2$ )	Average Size ( $\mu\text{m}$ )
L001	2902	11511	3.96
L005	1201	13062	9.87
L010	2334	14355	6.15
L015	2350	9800	4.17
L020	2241	7757	3.46
L025	1452	9385	6.46
L030	1284	9631	7.50
L035	1451	9630	6.63
L040	1505	8220	5.46
L045	1611	9095	5.64
L050	550	10488	10.07

Table 4.3: FSW Weld Nugget SiC particle counts and average size.

MICRO-ZONE	AVERAGE COUNT	AVERAGE SIZE ( $\mu\text{m}$ )	VOLUME ( $\mu\text{m}^3$ )
Weld Nugget	9233	6.7	334.14

Table 4.4 shows the summarized data of the fine SiC particles distribution and size. The weld nugget consist fine SiC particles ranging between 0.2 and 0.3 micron. The average count and the average size of the SiC particles in the three-dimensional microstructure are tabulated in Table 4.5. Based on the data obtained, it suggests the presence of two types of SiC particles: fine particles 0.2 and 0.3 in size, and coarse particles between 1 and 10 micron in size.

Table 4.4: Summary of FSW Weld Nugget fine SiC particles distribution and size

Slice	Count	Total Area ( $\mu\text{m}^2$ )	Average Size ( $\mu\text{m}$ )
L001	13518	3161	0.23
L005	4078	873	0.21
L010	7022	1821	0.26
L015	9270	2317	0.25
L020	11180	2676	0.24
L025	3919	1096	0.28
L030	2962	809	0.27
L035	3417	924	0.27
L040	5911	1472	0.25
L045	4904	1278	0.26
L050	1239	393	0.32

Table 4.5: FSW Weld Nugget fine SiC particle counts and average size.

MICRO-ZONE	AVERAGE COUNT	AVERAGE SIZE ( $\mu\text{m}$ )	VOLUME ( $\mu\text{m}^3$ )
Weld Nugget	320925	0.27	80087.5

Using 1 micron diamond paste during polishing produced dirty microstructure images (Figure 5.1 (a)) and the alignment process for three-dimensional reconstruction cannot be done smoothly and very time consuming due to the manual alignment and image editing. While using 0.25 micron diamond paste during polishing produced very clear microstructure images (Figure 5.1 (b)) but it consumed 30 minutes for only 0.5 micron thickness to be removed compare using 1 micron diamond paste which required only 10 minutes for 1 micron thickness removal.

The polishing shall involve using both diamond pastes where the 1 micron diamond paste is for the 0.75 micron thickness removal between 7 to 8 minutes polishing time. While the 0.25 diamond paste for the rest 0.25 micron thickness removal between 10 to 12 minutes polishing time to obtain clear and distinct microstructure images. Thus, the three-dimensional reconstruction can be done smoothly and the three-dimensional image produced will be clearer and ease the characterization of material process.

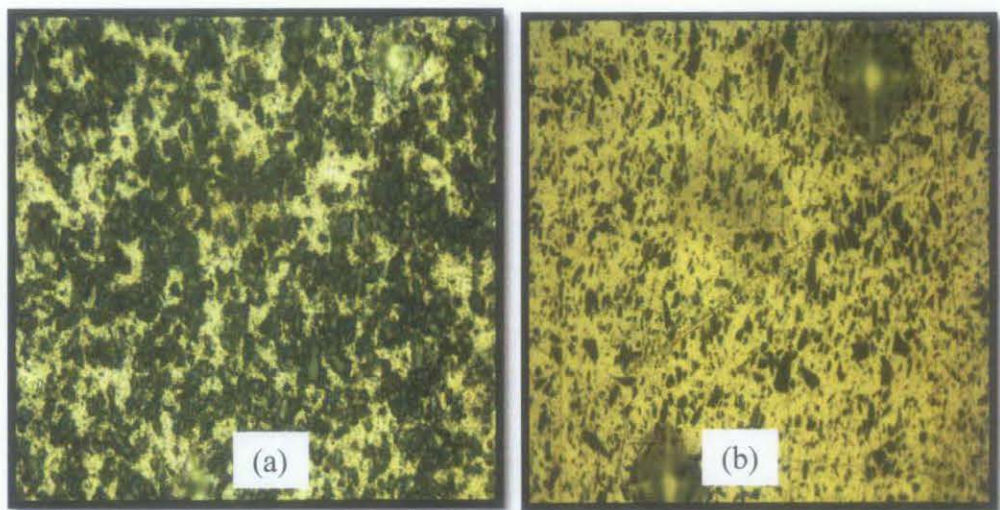


Figure 5.1: (a) Sample polished using 1 micron diamond paste (b) Sample polished using 0.25 micron diamond paste.

In this project, only one spot of the weld nugget being reconstruct. More spots of the weld nugget shall be considered for more conclusive results. The other micro-zones like base metal, HAZ and TMAZ zone also relevant to be three-dimensional reconstructed so the different effect due to friction stir welding can be studied.

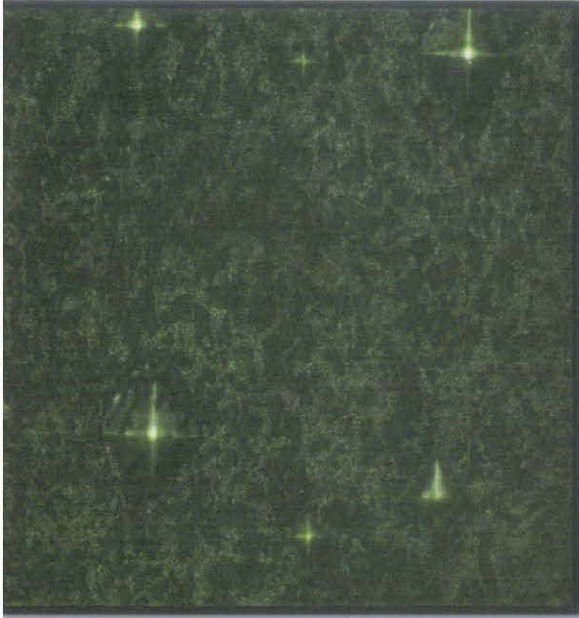
## REFERENCES

1. M.V. Kral, University of Canterbury, Christchurch, New Zealand, Gene Ice and M.K. Miller, Oak Ridge National Laboratory, M.D. Uchic, Wright-Patterson Air Force Research Laboratory, R.O. Rosenberg, Naval Research Laboratory, 2004, "Three-Dimensional Microscopy".
2. Cornelius A. Johnson, 2000, "Metallography Principles and Procedures Leco Corporation"
3. Won Bae Lee, Yun Mo Yeon, Shae K. Kim, Young-Jig Kim and Seong Boo Jung, "Microstructure and Mechanical Properties of Friction Stir Welded AZ31 MG Alloy"
4. 2001."Space Shuttle Technology Summary: Friction Stir Welding" , Pub 8-1263, FS-2001-03-60-MSFC
5. M.V Kral, M.A Mangan, G. Spanos and R.O Rosenberg, 2000 "Material Characterization" Volume 45 Page 17-25.
6. Manoj Kumar Shivaraj, Venkatesh Mahadevanand Vijay Dinakaran, 2010 "Frictional Stir Welding on Aluminum Alloys AA2024-T4 and AA7075-T6" Volume 5
7. H.J. McQueen, M. Cabibbo, E. Evangelista, S. Spigarelli, M. Di Paola, A. Falchero, Metallurgy Science and Material, "Microstructure And Mechanical Properties Of AA6056 Friction Stir Welded Plate" Page 22-30
8. Joseph Spacek and John Fiala, "Serial Section Electron Microscopy and Three Dimensional Reconstruction"
9. Govind Nandipati, Nageswara Rao Damera, Ramanainah Nallu, 2010 "Effects of Microstructural changes on Mechanical Properties of Friction Stir Welded Nano SiC Reinforced AA6061 Composite" International Journal of Engineering Science and Technology, Volume 2 Page 6491-6499.

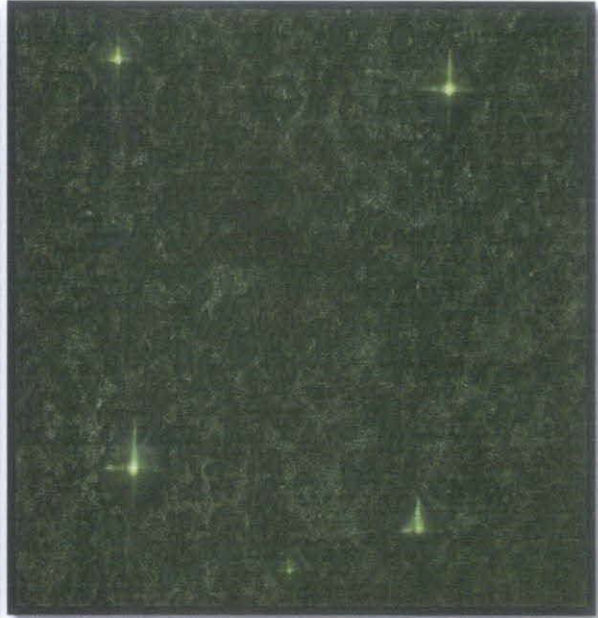
10. J.A. Lee, R.W. Carter and J. Ding, 1999 "Friction Stir Welding for Aluminum Metal Matrix Composites (MMC's)" MSFC Center Director's Discretionary Fund Final Report, Project No. 98-09.
11. M. Kathiresan and T. Sornakumar, 2010 "EDM Studies on Aluminum Alloy-Silicon Carbide Composite Developed by Vortex Technique and Pressure Die-Casting" Journal of Minerals and Materials Characterization and Engineering, Volume 9 Page 79-88.
12. Iuri Boromei, Lorella Ceschini, Allessandro Morri and Gian Luca Garagani, 2005 "Friction Stir Welding of Aluminum Based Composites Reinforced with Al<sub>2</sub>O<sub>3</sub> Particles: Effects on Microstructure and Charpy Impact Energy" Metallurgy Science and Technology, Page 12-21.
13. D. Storjohan, S.S. Babu, S.A. David and Phil Sklad, 2005 "Friction Stir Welding of Aluminum Metal Matrix Composites"
14. Huseyin Uzun, 2007 "Friction stir welding of SiC particulate reinforced AA2124 aluminium alloy matrix composite" Material and Design, Volume 28, Issue 25.
15. [http://www.google.com.my/imglanding?imgurl=http://www.metallographic.com/Images/METACUTM.jpg&imgrefurl=http://picsicio.us/domain/metallographic.com/&h=377&w=360&sz=52&tbid=3jZSoyGBDK6guM:&tbnh=122&tbnw=116&prev=/images%3Fq%3Dabrasive%2Bcutter&zoom=1&q=abrasive+cutter&hl=en&usg=\\_\\_lDsSAqDwLqJ0i4zBZYUkG\\_in\\_Ho%3D&sa=X&ei=monNTOX\\_LoOmvgOjqtz3Dw&ved=0CCMQ9QEwAQ](http://www.google.com.my/imglanding?imgurl=http://www.metallographic.com/Images/METACUTM.jpg&imgrefurl=http://picsicio.us/domain/metallographic.com/&h=377&w=360&sz=52&tbid=3jZSoyGBDK6guM:&tbnh=122&tbnw=116&prev=/images%3Fq%3Dabrasive%2Bcutter&zoom=1&q=abrasive+cutter&hl=en&usg=__lDsSAqDwLqJ0i4zBZYUkG_in_Ho%3D&sa=X&ei=monNTOX_LoOmvgOjqtz3Dw&ved=0CCMQ9QEwAQ)

# APPENDIX I

## SERIAL SECTIONING 2D IMAGES



L001



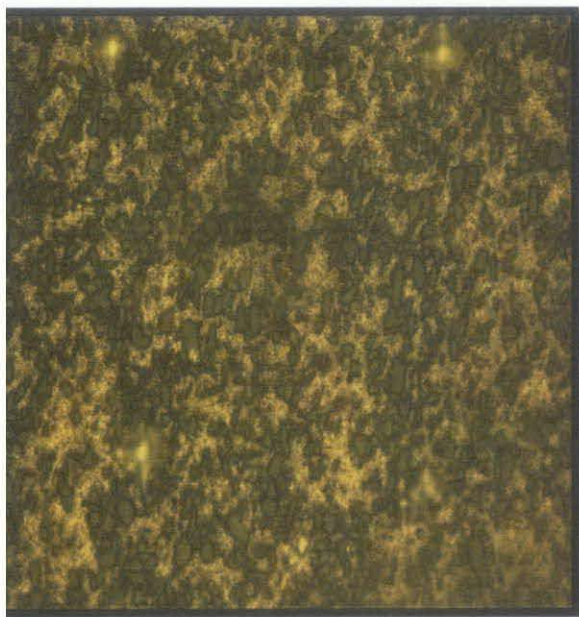
L002



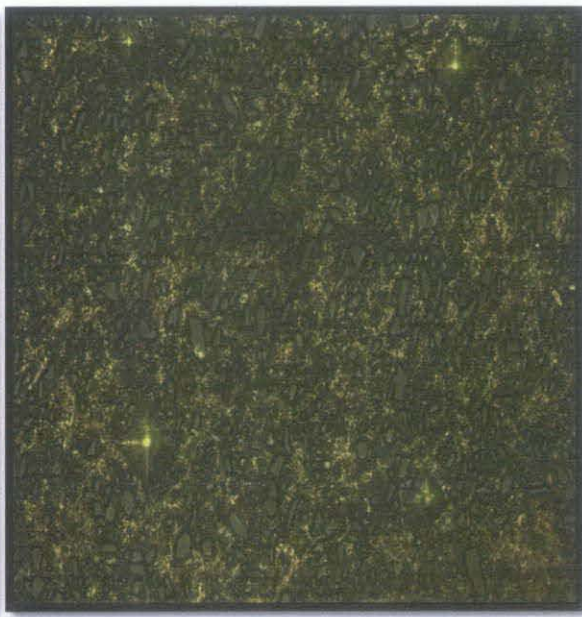
L003



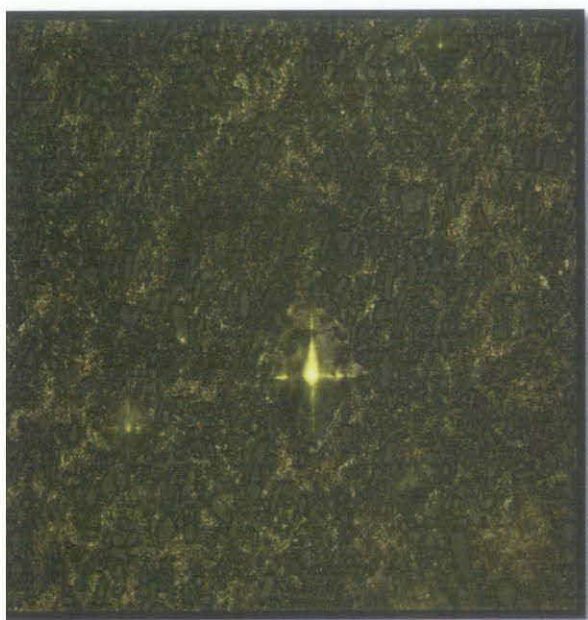
L004



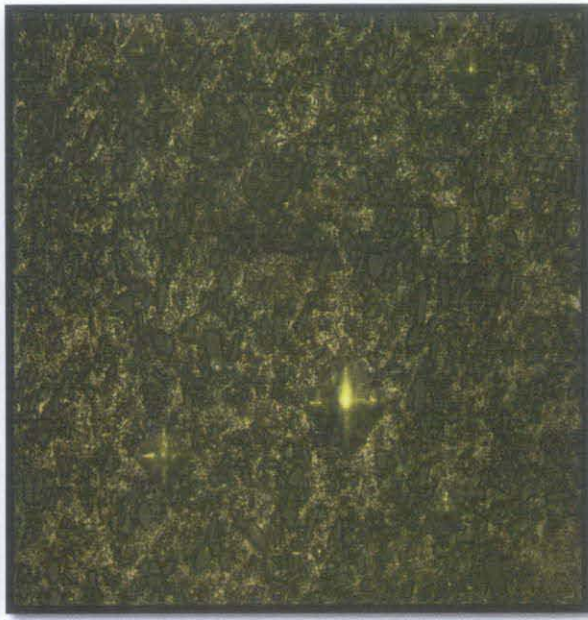
L005



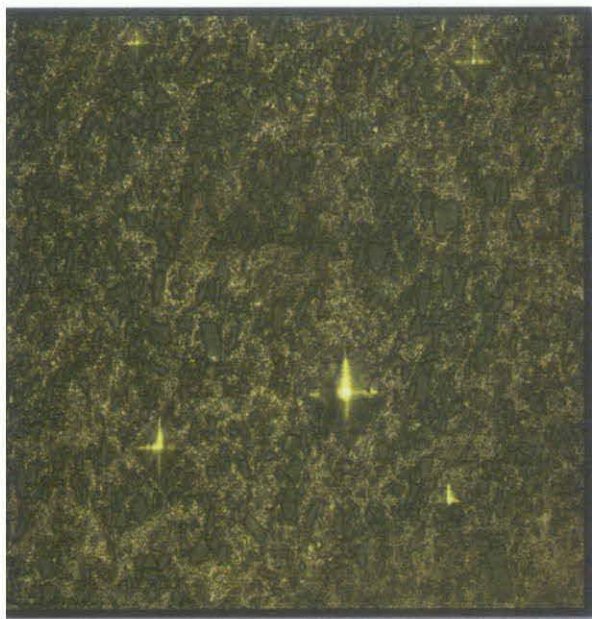
L006



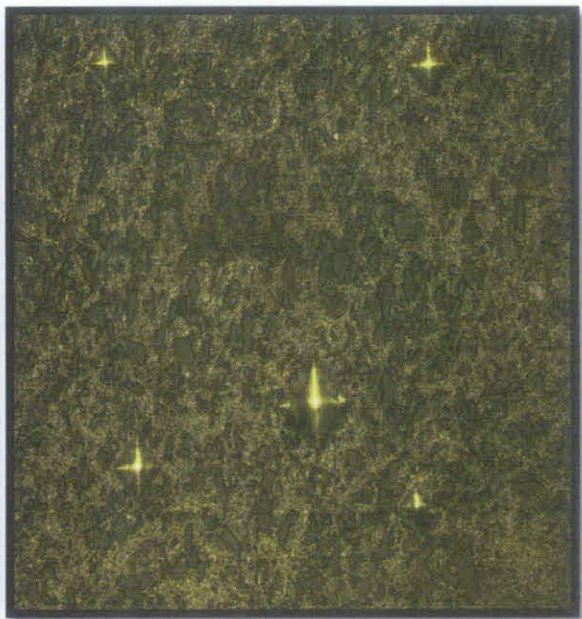
L007



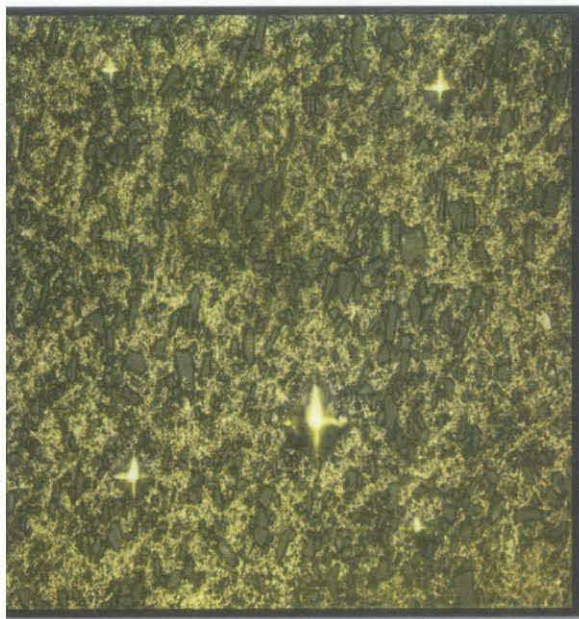
L008



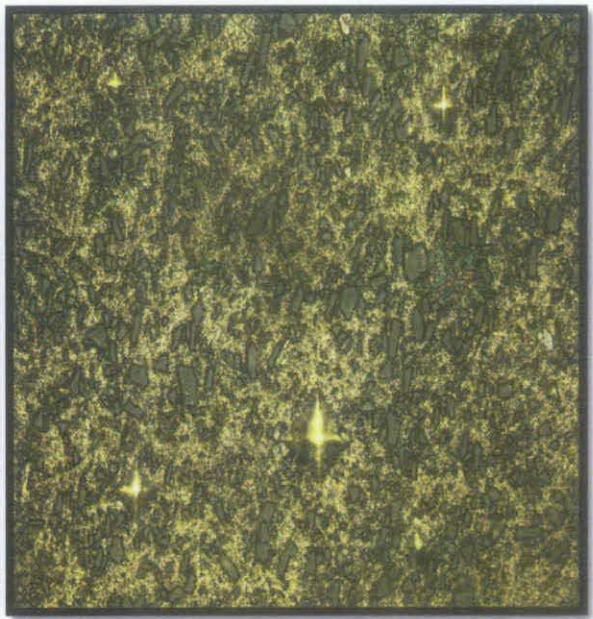
L009



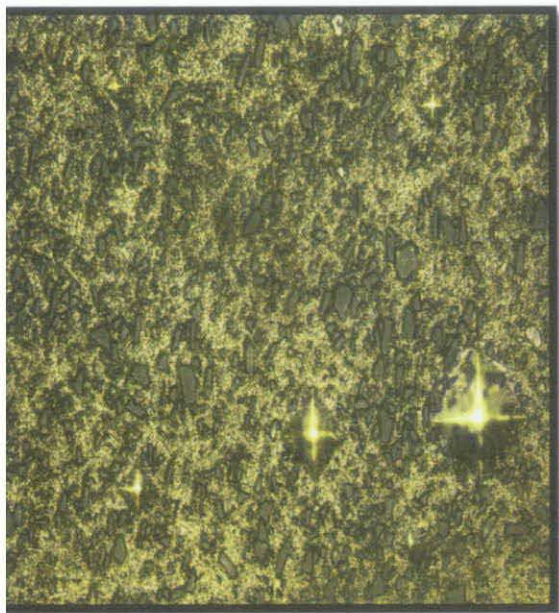
L010



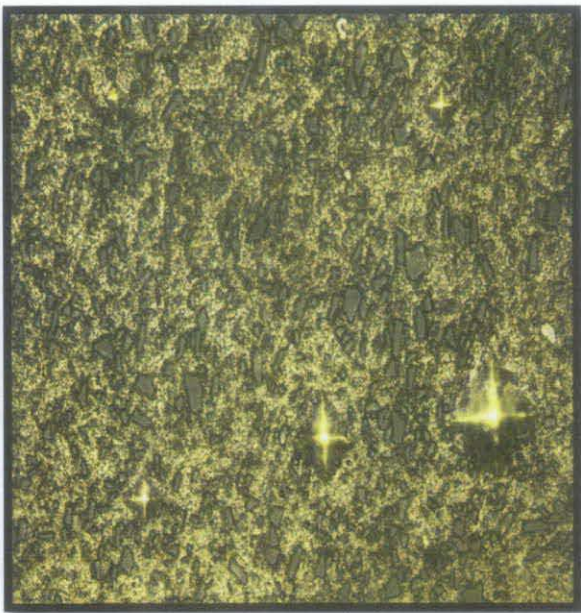
L011



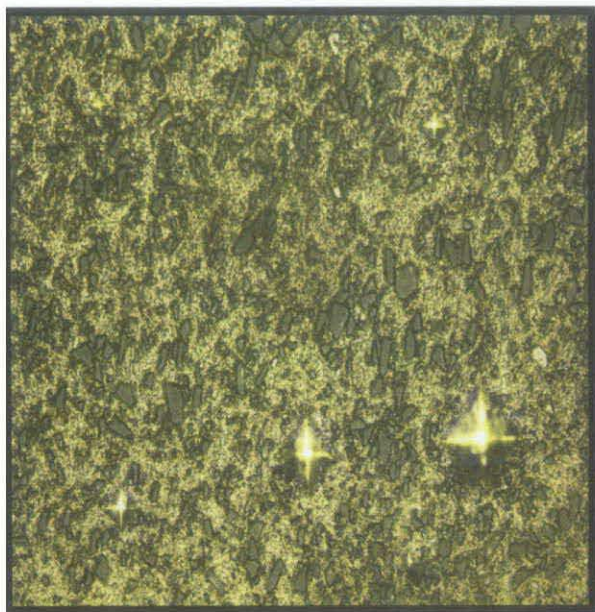
L012



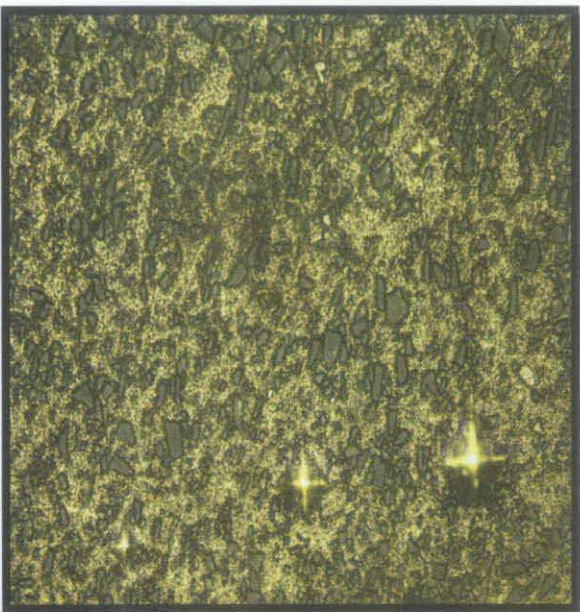
L013



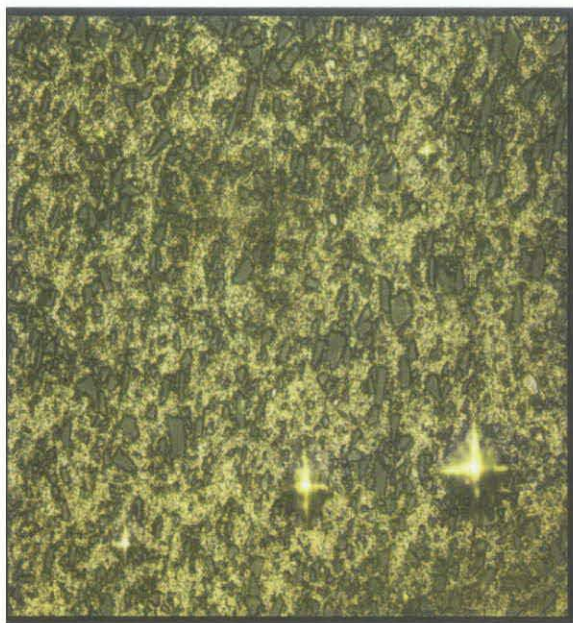
L014



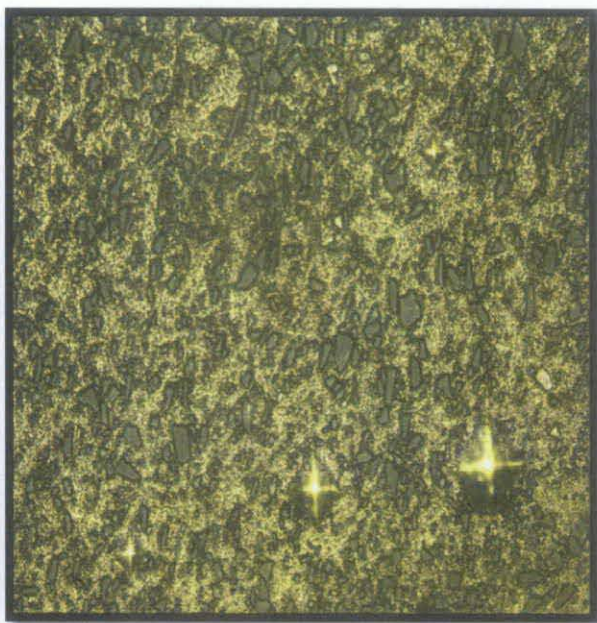
L015



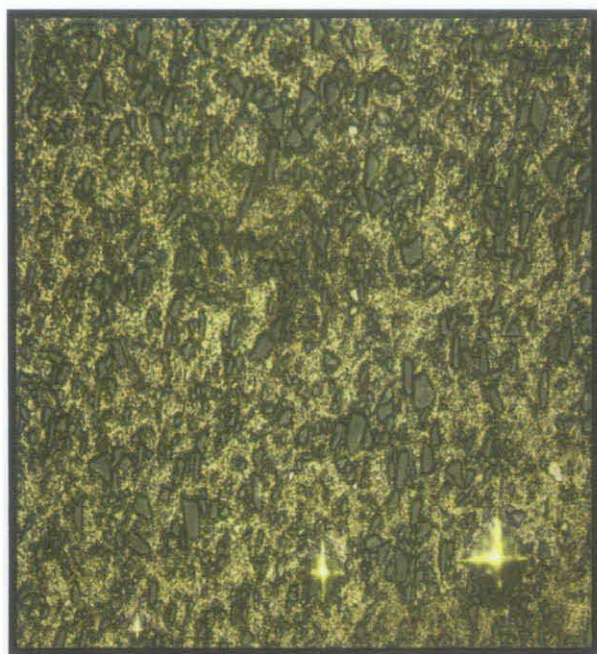
L016



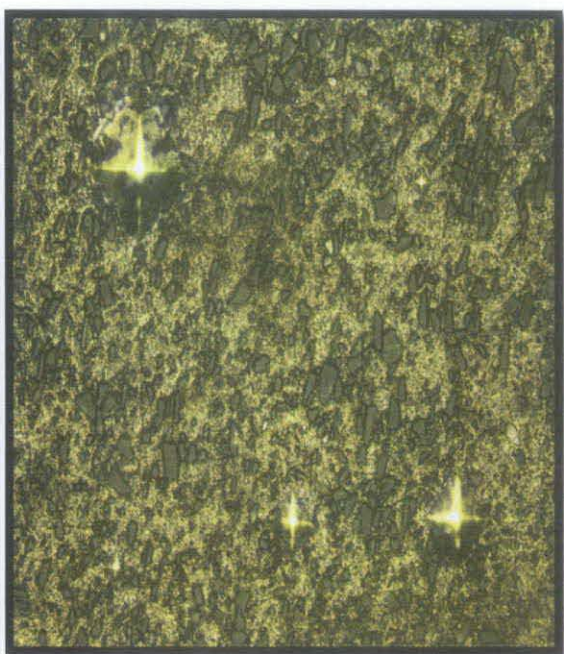
L017



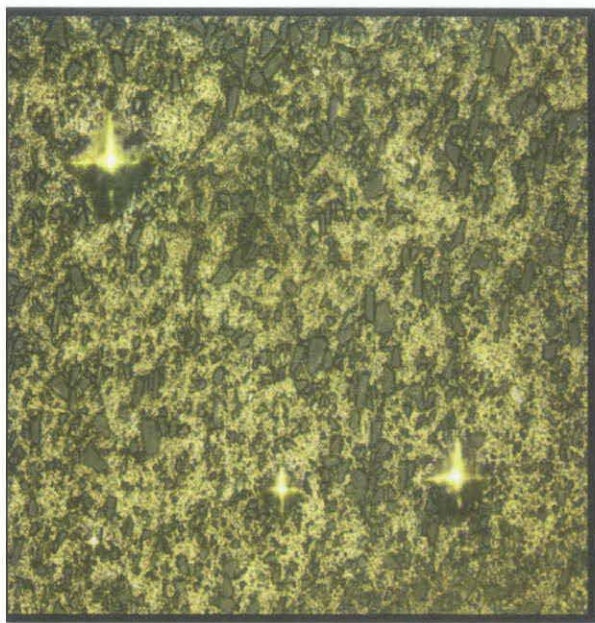
L018



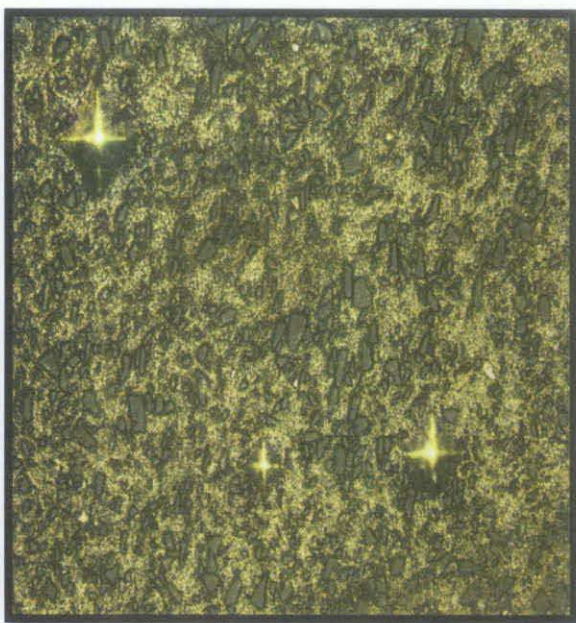
L019



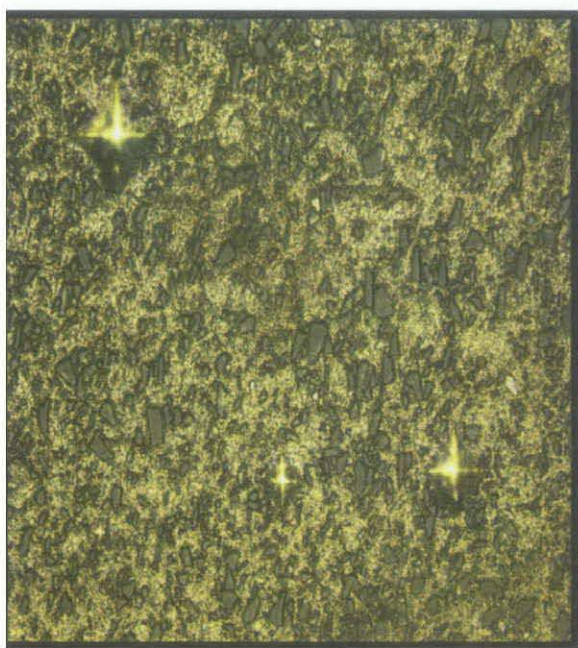
L020



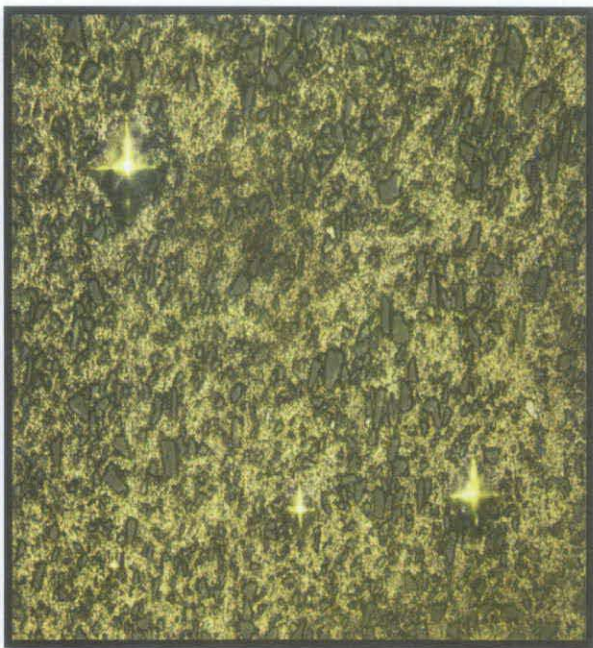
L021



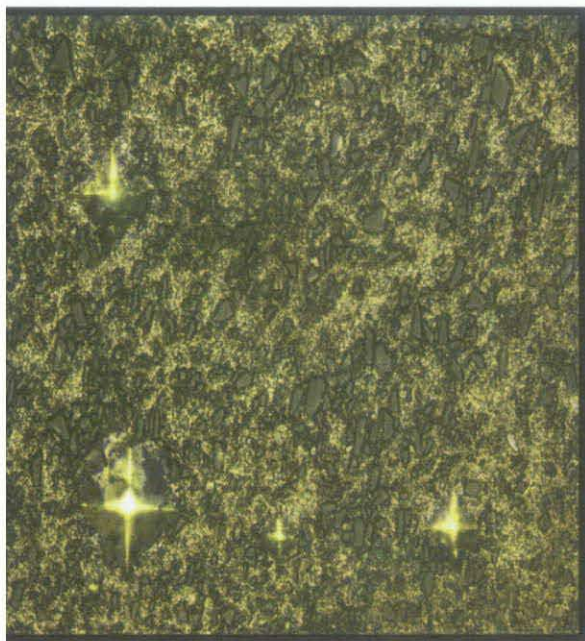
L022



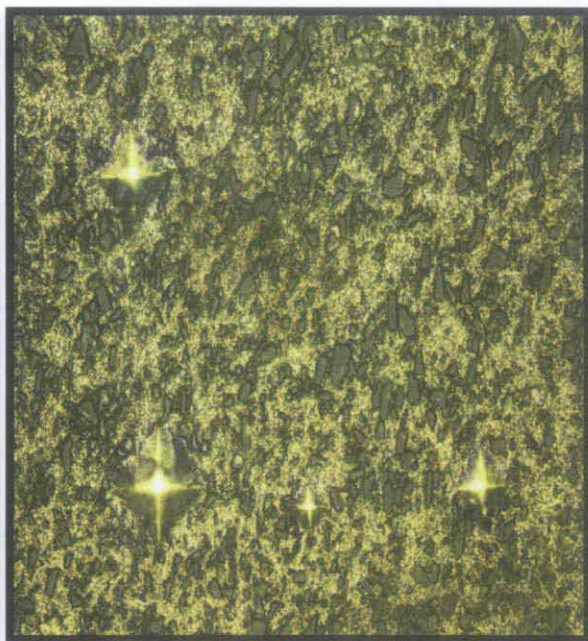
L023



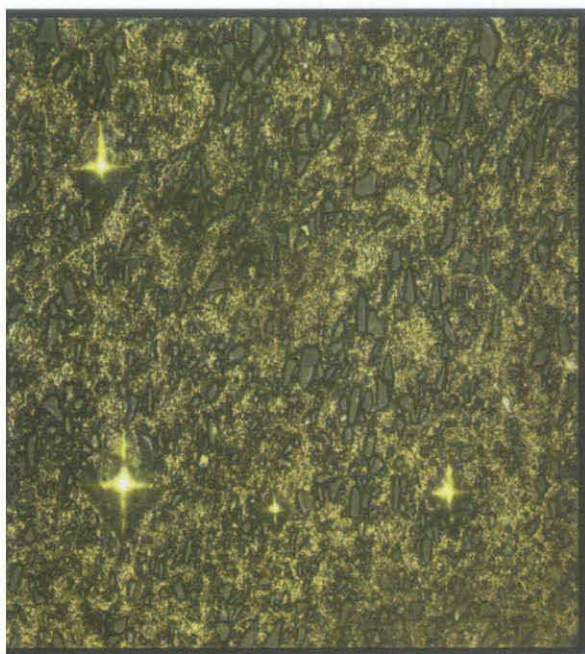
L024



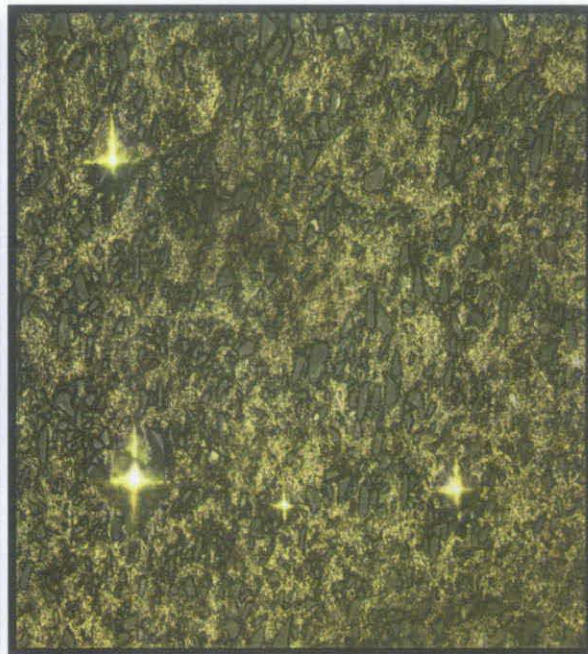
L025



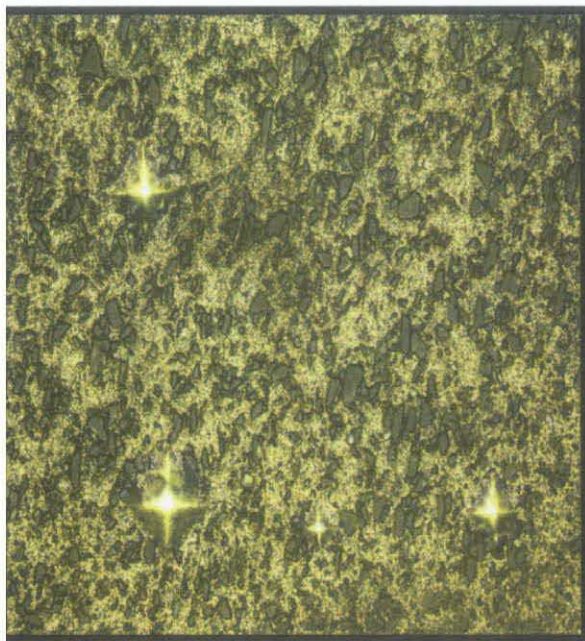
L026



L027



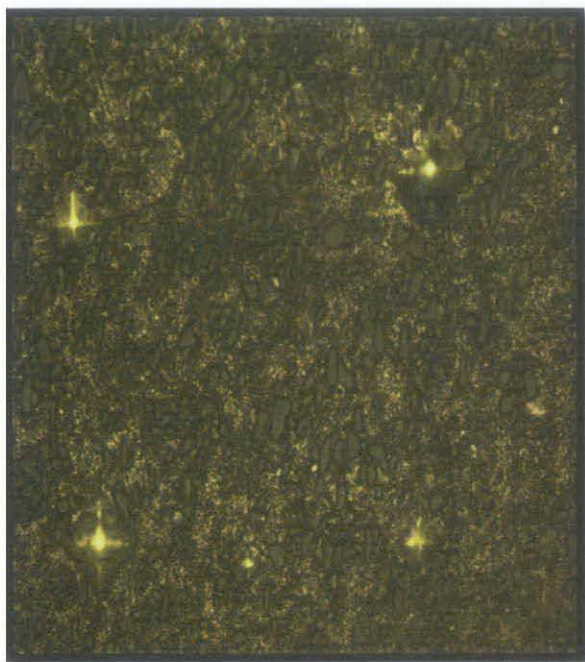
L028



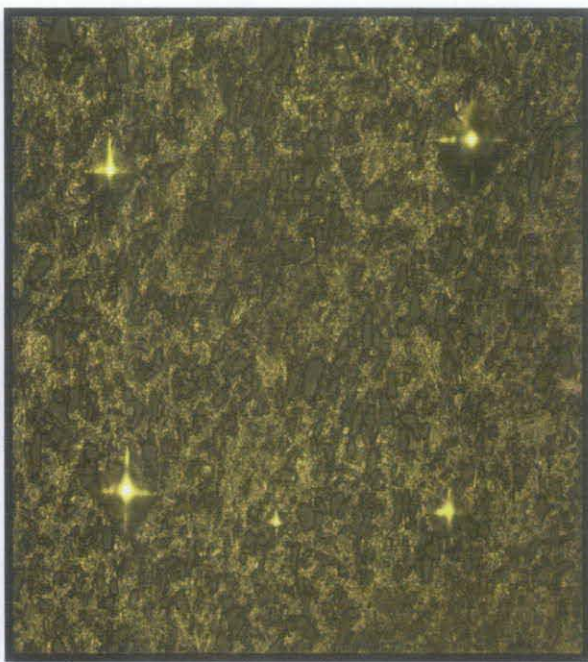
L029



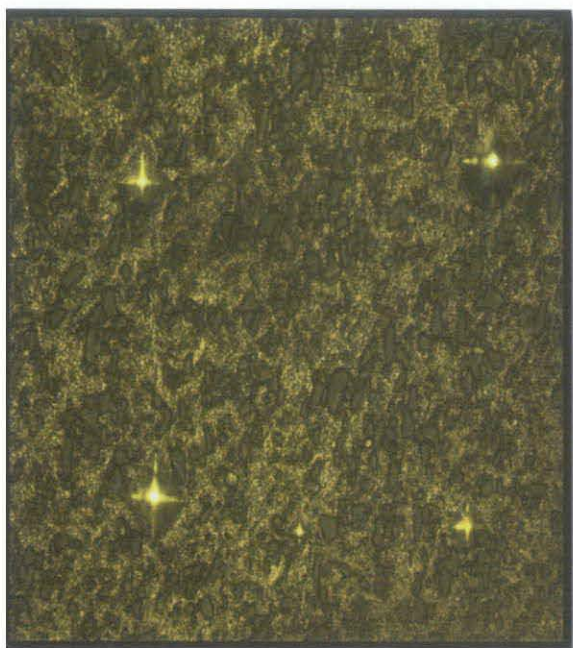
L030



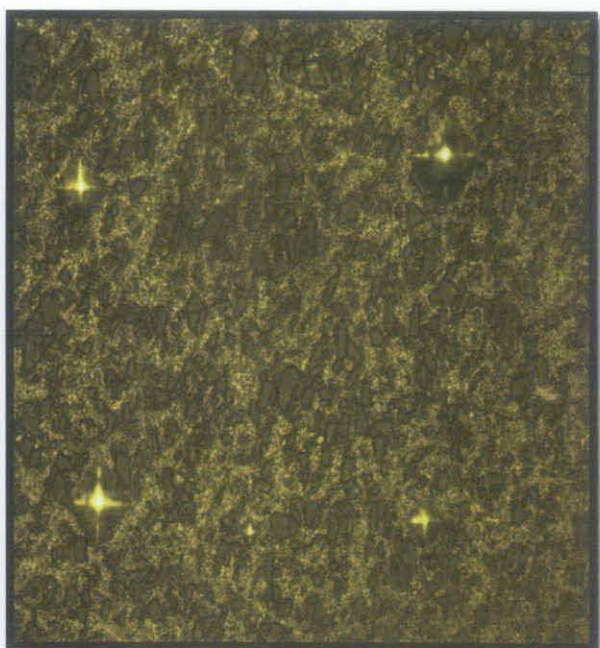
L031



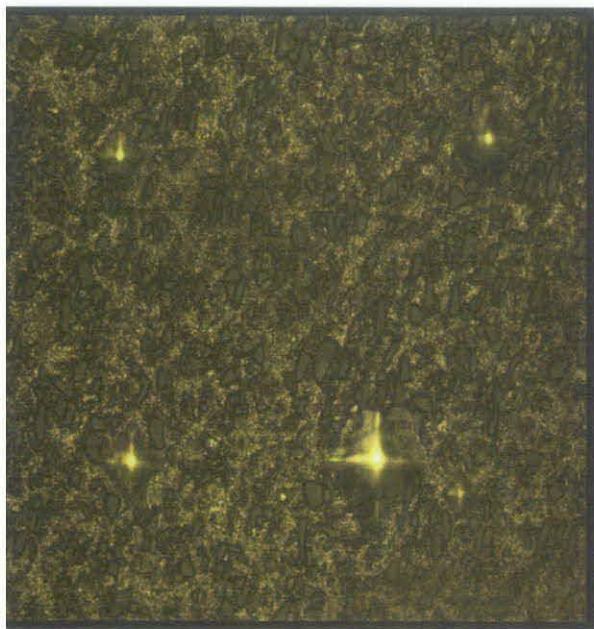
L032



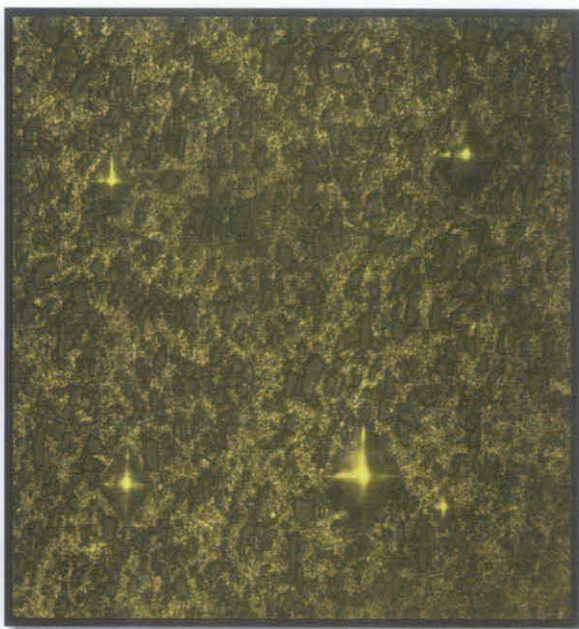
L033



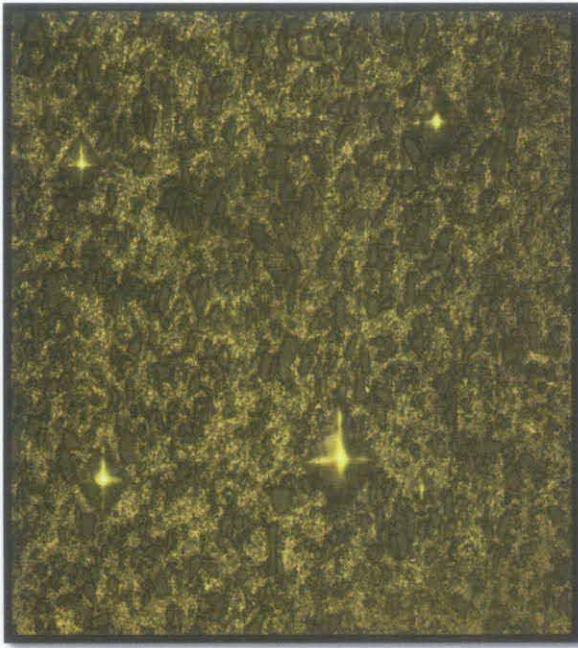
L034



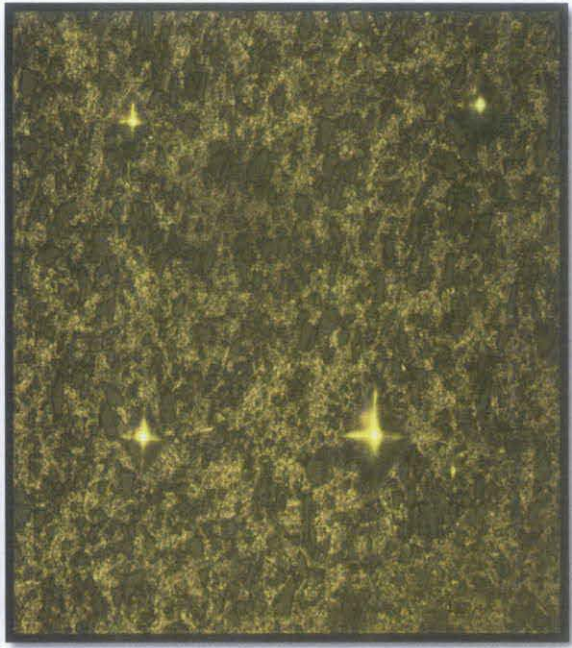
L035



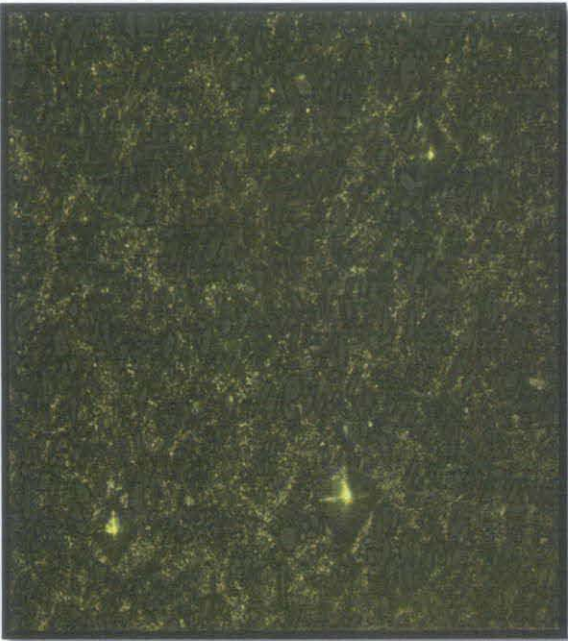
L036



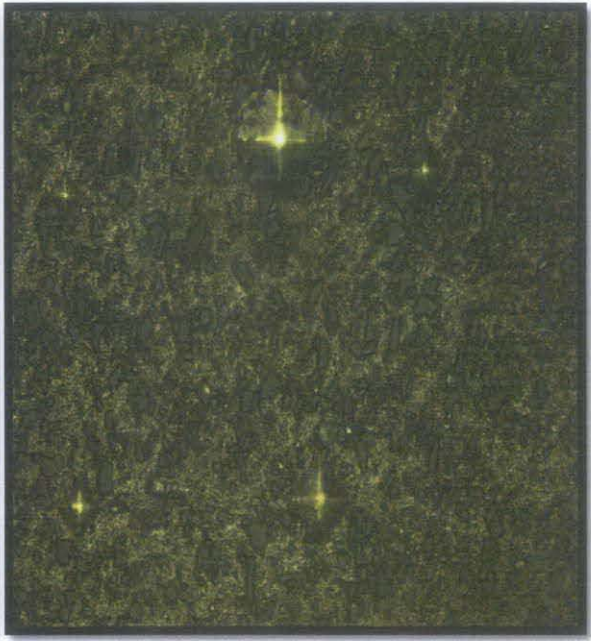
L037



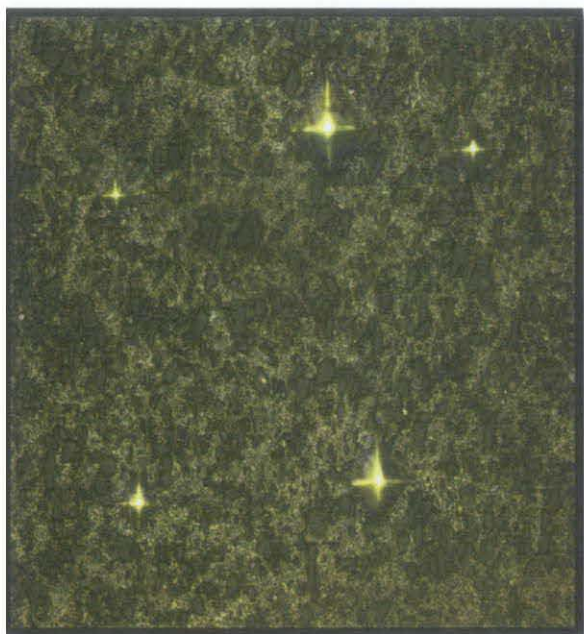
L038



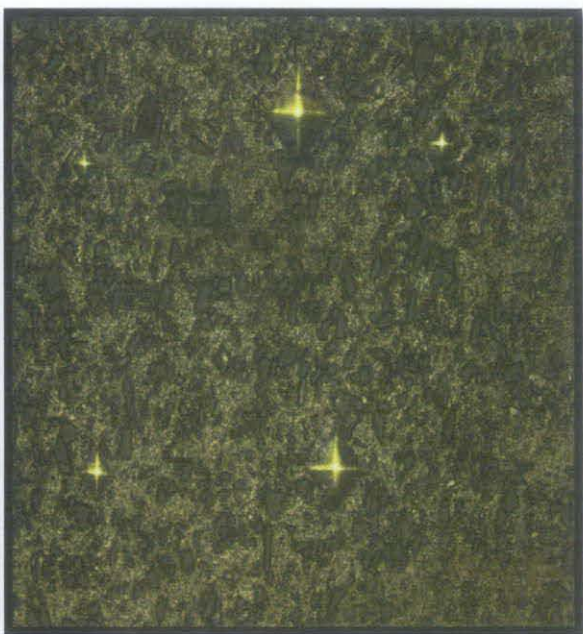
L039



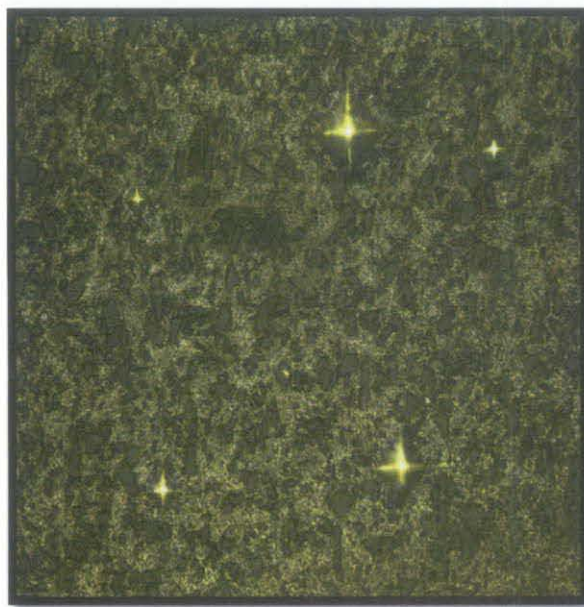
L040



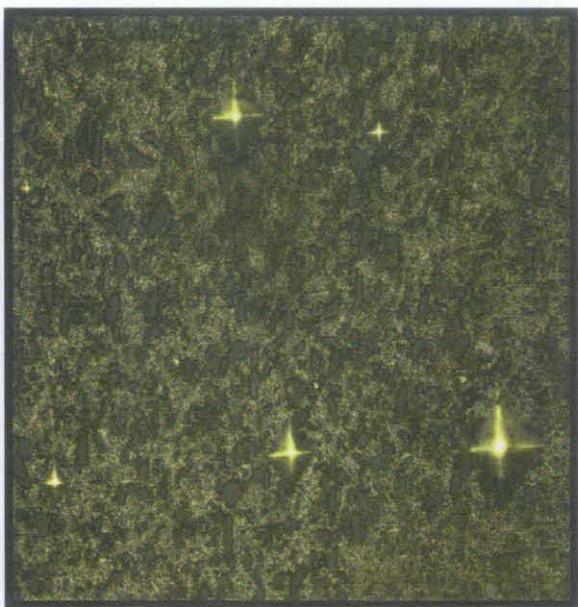
L041



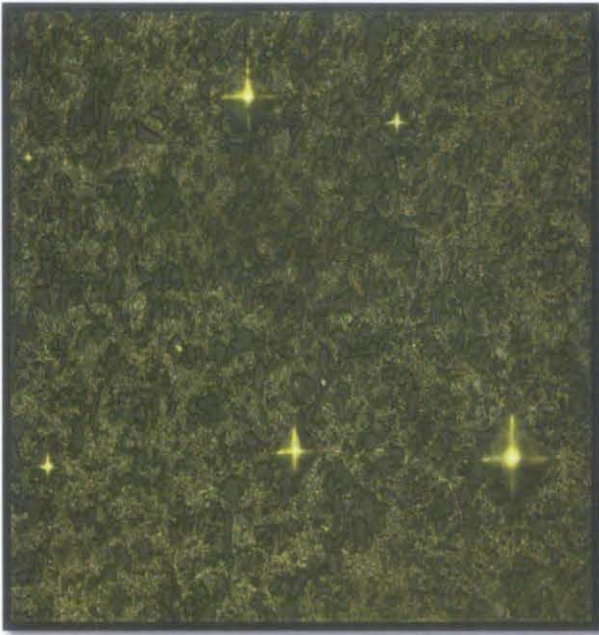
L042



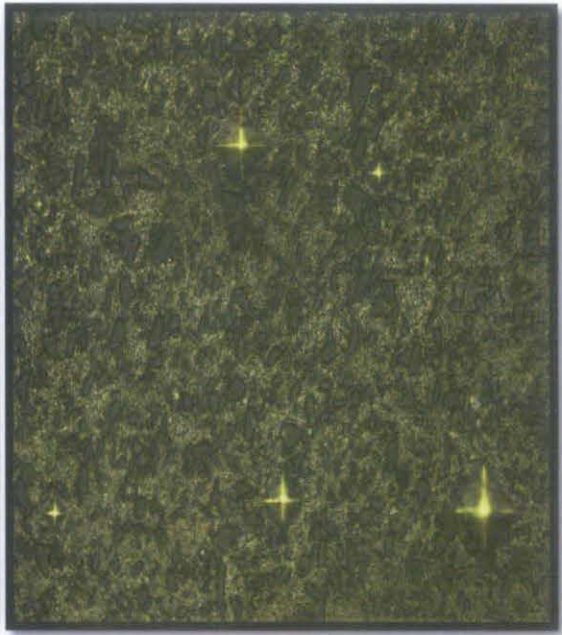
L043



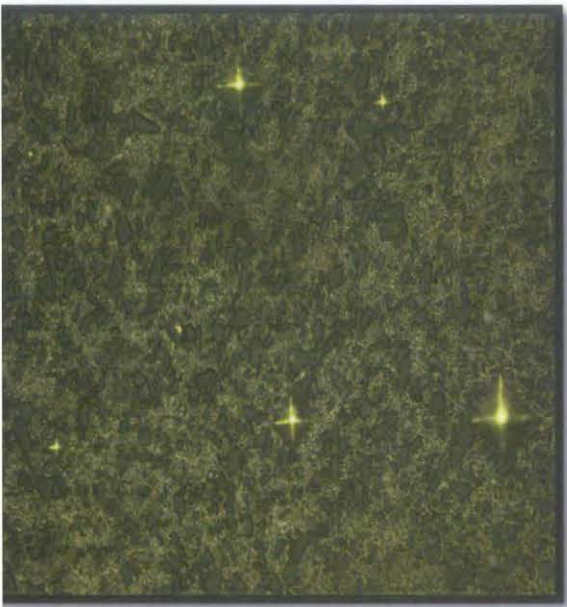
L044



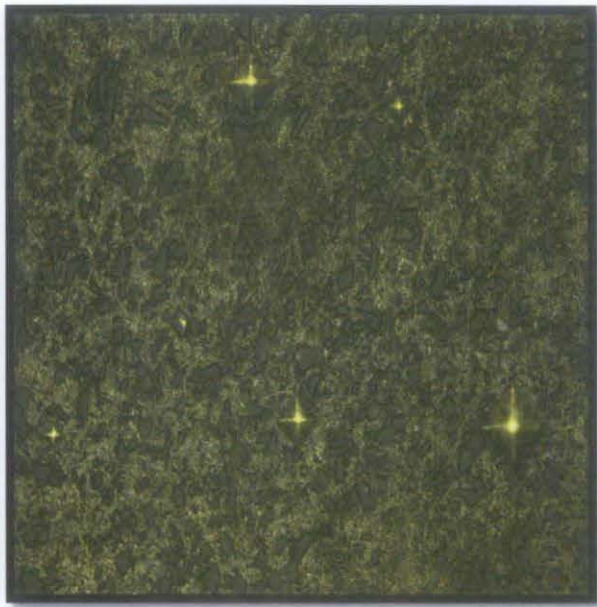
L045



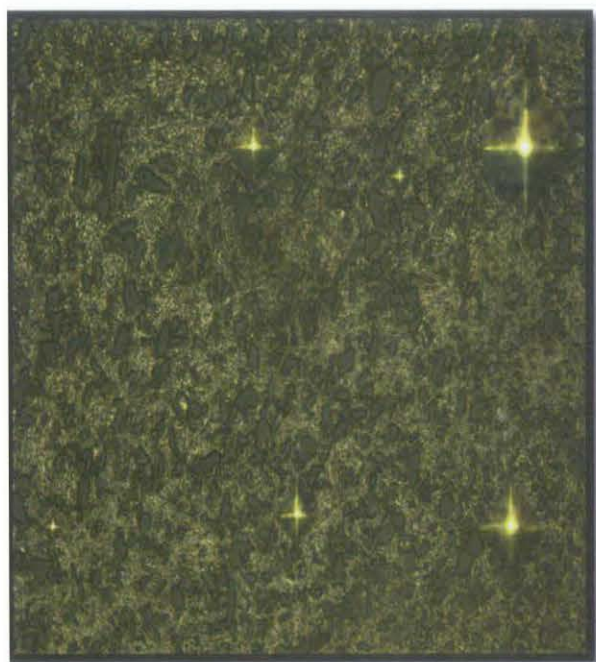
L046



L047



L048



L049



L050

## APPENDIX 2

### FSW WELD NUGGET COARSE SiC PARTICLES DISTRIBUTION AND SIZE

Slice	Count	Total Area	Average Size
L001	2902	11511.229	3.967
L002	2343	10059.555	4.293
L003	2736	12549.818	4.587
L004	2458	8696.93	3.538
L005	1201	13062.472	10.876
L006	2179	10498.353	4.818
L007	2179	7244.655	3.325
L008	2506	8142.278	3.249
L009	2812	9027.524	3.21
L010	2334	14355.339	6.151
L011	2466	8092.794	3.282
L012	1727	4888.307	2.831
L013	2483	8166.405	3.289
L014	2132	6160.763	2.89
L015	2350	9800.277	4.17
L016	1387	8828.987	6.366
L017	1554	8777.345	5.648
L018	1276	10521.988	8.246
L019	1921	6571.307	3.421
L020	2241	7757.091	3.461
L021	1988	6510.156	3.275
L022	1740	8612.744	4.95
L023	2214	7544.864	3.408
L024	1776	8115.063	4.569
L025	1452	9385.989	6.464
L026	2269	7941.993	3.5
L027	1391	10239.839	7.361
L028	1168	11377.15	9.741
L029	1048	11364.881	10.844
L030	1284	9631.277	7.501
L031	1001	8061.126	8.053
L032	1855	10806.022	5.825
L033	1366	12069.215	8.835
L034	1667	10104.257	6.061
L035	1451	9630.348	6.637
L036	1758	10376.405	5.902
L037	1137	9361.534	8.234
L038	2043	9644.912	4.721

L039	1292	6727.929	5.207
L040	1505	8220.398	5.462
L041	779	10056.222	12.909
L042	1345	10053.161	7.474
L043	380	9706.528	25.543
L044	459	8758.436	19.082
L045	1611	9095.288	5.646
L046	693	7903.548	11.405
L047	488	8995.063	18.433
L048	1095	8537.166	7.796
L049	792	7614.978	9.615
L050	550	10488.899	19.071

### APPENDIX III

#### FSW WELD NUGGET FINE SiC PARTICLES DISTRIBUTION AND SIZE

Slice	Count	Total Area	Average Size
L001	13518	3161.452	0.234
L002	8517	2113.682	0.248
L003	9381	2344.161	0.25
L004	10767	2619.67	0.243
L005	4078	873.77	0.214
L006	7206	2020.48	0.28
L007	13079	3182.355	0.243
L008	13557	3208.996	0.237
L009	14850	3527.567	0.238
L010	7022	1821.233	0.259
L011	14486	3317.746	0.229
L012	20844	4294.117	0.206
L013	13706	3210.526	0.234
L014	14709	3280.066	0.223
L015	9270	2317.274	0.25
L016	2963	916.914	0.309
L017	3509	1028.725	0.293
L018	2638	822.974	0.312
L019	8632	2083.134	0.241
L020	11180	2676.149	0.239
L021	12523	2917.967	0.233
L022	5059	1406.808	0.278
L023	10846	2579.613	0.238
L024	5142	1425.443	0.277
L025	3919	1096.488	0.28
L026	9875	2420.559	0.245
L027	3625	1025.582	0.283
L028	2456	769.228	0.313
L029	2516	768.736	0.306
L030	2962	809.258	0.273
L031	1390	432.404	0.311
L032	5104	1310.491	0.257
L033	3071	843.003	0.275
L034	4247	1103.729	0.26
L035	3417	924.21	0.27
L036	4788	1225.376	0.256
L037	2348	691.436	0.294
L038	6013	1633.926	0.272

L039	3101	991.455	0.32
L040	5911	1472.113	0.249
L041	1453	453.853	0.312
L042	3547	994.624	0.28
L043	546	153.917	0.282
L044	861	255.672	0.297
L045	4904	1278.521	0.261
L046	1285	425.955	0.331
L047	836	241.135	0.288
L048	2331	712.312	0.306
L049	1698	508.829	0.3
L050	1239	393.822	0.318

## APPENDIX III

### FSW WELD NUGGET FINE SiC PARTICLES DISTRIBUTION AND SIZE

Slice	Count	Total Area	Average Size
L001	13518	3161.452	0.234
L002	8517	2113.682	0.248
L003	9381	2344.161	0.25
L004	10767	2619.67	0.243
L005	4078	873.77	0.214
L006	7206	2020.48	0.28
L007	13079	3182.355	0.243
L008	13557	3208.996	0.237
L009	14850	3527.567	0.238
L010	7022	1821.233	0.259
L011	14486	3317.746	0.229
L012	20844	4294.117	0.206
L013	13706	3210.526	0.234
L014	14709	3280.066	0.223
L015	9270	2317.274	0.25
L016	2963	916.914	0.309
L017	3509	1028.725	0.293
L018	2638	822.974	0.312
L019	8632	2083.134	0.241
L020	11180	2676.149	0.239
L021	12523	2917.967	0.233
L022	5059	1406.808	0.278
L023	10846	2579.613	0.238
L024	5142	1425.443	0.277
L025	3919	1096.488	0.28
L026	9875	2420.559	0.245
L027	3625	1025.582	0.283
L028	2456	769.228	0.313
L029	2516	768.736	0.306
L030	2962	809.258	0.273
L031	1390	432.404	0.311
L032	5104	1310.491	0.257
L033	3071	843.003	0.275
L034	4247	1103.729	0.26
L035	3417	924.21	0.27
L036	4788	1225.376	0.256
L037	2348	691.436	0.294
L038	6013	1633.926	0.272

L039	3101	991.455	0.32
L040	5911	1472.113	0.249
L041	1453	453.853	0.312
L042	3547	994.624	0.28
L043	546	153.917	0.282
L044	861	255.672	0.297
L045	4904	1278.521	0.261
L046	1285	425.955	0.331
L047	836	241.135	0.288
L048	2331	712.312	0.306
L049	1698	508.829	0.3
L050	1239	393.822	0.318